Accepted Manuscript

New isoxazolidinone and 3,4-dehydro-β-proline derivatives as antibacterial agents and MAO-inhibitors: A complex balance between two activities

Lucia Ferrazzano, Angelo Viola, Elena Lonati, Alessandra Bulbarelli, Rosario Musumeci, Clementina Cocuzza, Marco Lombardo, Alessandra Tolomelli

PII: S0223-5234(16)30735-8

DOI: 10.1016/j.ejmech.2016.09.007

Reference: EJMECH 8873

To appear in: *European Journal of Medicinal Chemistry*

Received Date: 26 July 2016

Revised Date: 1 September 2016

Accepted Date: 2 September 2016

Please cite this article as: L. Ferrazzano, A. Viola, E. Lonati, A. Bulbarelli, R. Musumeci, C. Cocuzza, M. Lombardo, A. Tolomelli, New isoxazolidinone and 3,4-dehydro-β-proline derivatives as antibacterial agents and MAO-inhibitors: A complex balance between two activities, *European Journal of Medicinal Chemistry* (2016), doi: 10.1016/j.ejmech.2016.09.007.

Journal

New isoxazolidinone and 3,4-dehydro-β-proline derivatives as antibacterial agents and MAO-inhibitors: a complex balance between two activities.

Lucia Ferrazzano[a], Angelo Viola[a], Elena Lonati[b], Alessandra Bulbarelli[b], Rosario Musumeci[b], Clementina Cocuzza[b], Marco Lombardo[a], Alessandra Tolomelli[a]*.

[a]*Department of Chemistry, University of Bologna, Via Selmi 2, 40126, Bologna, Italy*
[b]*Department of Medicine and Surgery, University of Milano-Bicocca, Via Cadore 48, 20900, Monza, Italy*

ABSTRACT

Among the different classes of antibiotics, oxazolidinone derivatives represent important drugs, since their unique mechanism of action overcomes commonly diffused multidrug-resistant bacteria. Anyway, the structural similarity of these molecules to monoamino oxidase (MAO) inhibitors, like toloxatone and blefoxatone, induces in many cases loss of selectivity as a major concern. A small library of compounds based on isoxazolinone and dehydro-β-proline scaffold was designed with the aim to obtain antibacterial agents, evaluating at the same time the potential effects of structural features on MAO inhibitory behaviour. The structural modification introduced in the backbone, starting from Linezolid model, lead to a significant loss in antibiotic activity, while a promising inhibitory effect could be observed on monoamino oxidases. These interesting results are also in agreement with docking experiments suggesting a good binding pose of the synthesized compounds into the pocket of the oxidase enzymes, in particular of MAO-B.

1. Introduction

The increase of phenomena of antibiotic resistance became a central matter in public health programs, since it represents a problem not only for people already infected, but also for the diffusion of resistant bacteria to other people.[1] The problem grew with the appearance of multidrug-resistant ESKAPE pathogens (*Enterococcus* spp, *Staphylococcus aureus, Klebsiella* spp, *Acinetobacter baumannii, Pseudomonas aeruginosa, Enterobacter* spp), usually causes of chronic infections like skin infections, meningitis, urogenital tract diseases and respiratory tract infections. This emergency justifies the continuous research for new type of antibiotics. Between the most recent classes of antibiotics, oxazolidinones represent a great innovation in the attempt of limiting the diffusion of "smartly" modified Gram-positive bacteria. Linezolid (Zyvox®) represents a well-known antimicrobial agent able to fight Vancomicyn-Resistant Enterococci (VRE), Methicillin-Resistant *Staphylococcus aureus* (MRSA) and Penicillin-Resistant *Streptococcus pneumoniae* (PNSSP).[2-3] Like other molecules belonging to the family of oxazolidinones, Linezolid's mechanism of action regards the binding to peptidyltransferase centre (PTC), corresponding to 50S subunit of prokaryotic ribosome. The structure of Linezolid consists in four chemical moieties that can justify its interaction with the ribosomal binding site (Figure 1). Ring-A is the pharmacokinetic oxazolidinone ring and interacts with fixed residues of the PTC pocket through van der Waals interactions. The acetamide NH on the tail participates in hydrogen bond with the phosphate group on a residue in the upper part of the pocket. The oxazolidinone fits, together with the C5-tail, in the direction of the ribosomal tunnel, orienting the ring-C toward the inter-subunit interface. Ring-B is sandwiched through π-staking with two residues and participates in a T-shaped interaction, while the C2 fluorine points out of the pocket to contribute to the coordination of a putative magnesium ion that appears upon Linezolid binding in this particular configuration. The morpholine in Ring-C, does not give particular interactions with the binding site but has great importance in the modulation of molecule pharmacokinetic.[4-5] Despite all these favourable features, there are several cases of resistance to Linezolid.[6]

Considering their efficacy and evaluating the chance to introduce modifications to reduce resistance effects, oxazolidinones were deeply studied in their structure-activity relationships (SAR) in order to identify bioisosters of each part of the molecule, in particular of Ring-A. These studies revealed that bioisosteric modifications on Ring-A should maintain i) an sp^2 centre directly linked to Ring-B, ii) an oxygen atom properly located and iii) a C5-chiral centre stereochemically defined carrying the acylaminomethyl chain.[7] These requirements were confirmed by the results in terms of inhibition of the

proliferation of resistant bacteria reported for dihydrofuran-2-one (a), tetrahydrofuran-2-one (b), pyrrolidin-2-one (c), 3-phenylisoxazoline (d), 3-phenylisoxazolidone (e) and 1,2,4-oxadiazole (f) derivatives.

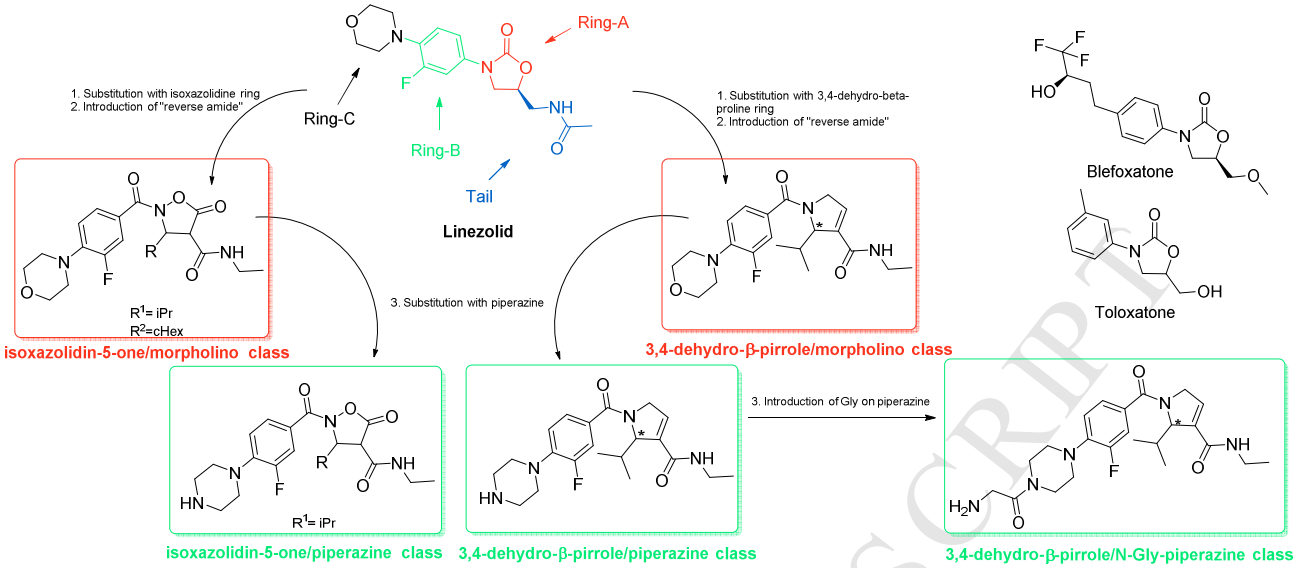

Figure 1. Structure of Linezolid and its analogues and structure of blefoxatone and toloxatone.

In vitro Minimum Inhibitory Concentration (MIC) microbiological tests, assessing the antibacterial activity, show how the gradually removal of one or more of the three features reported above results in decrease of antimicrobial activity (Figure 2). [8-9-10-11]

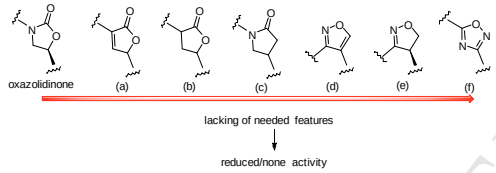

Figure 2. Bioisoster of Ring-A classified on the base of reduction of activity.

The few trials to change Ring-B did not give significant improvements in terms of activity, while several examples of changes in Ring-C are reported in literature and regard four major conceptual frameworks like fusion of ring B and C, separation of ring-B and C by a spacer, appendage of stabilizing moieties on Ring-C and new Ring-C. [10-12] Taking into account that the principal metabolites of Linezolid are produced during the lactone or lactame pathways, regarding so the morpholine ring oxidation,[13-14-15] a widely used substitution is piperazine and its derivatives, as reported for Eperezolid and its analogues. Usually, Linezolid analogues have a C5 aminomethyl functionalized tail as amide, urea and thiourea. With these moieties, the resulting structures are quite similar to those of monoamino oxidase (MAO) inhibitors, like toloxatone and blefoxatone (Figure 1), that are active against the two human isoforms of monoamino oxidase (MAO-A and MAO-B), responsible for the metabolism of monoamino neurotrasmitters.[16] In particular, MAO-A inhibitors have been successfully applied as anti-depressant, while molecule that are able to modulate MAO-B activity have been used in the treatment of Parkinson's disease and they are now receiving great attention for the protective effect on vascular and neuronal tissues, thus suggesting their possible use in the prevention and retard of Alzheimer's disease.[17]

These molecules convert amines into imines through the reduction of the cystinyl-FAD cofactor of MAO, then reoxidized by H_2O_2. The presence of ligands close to FAD influences the bioactivity: if the ligand is a MAO-inhibitor, the reduction of FAD goes through an anionic semiquinone intermediate to the fully reduced form and no reoxidation of FAD is observed; if the ligand is not an inhibitor, no intermediate is detected and only the fully reduced form of FAD can be observed.[18] Linezolid shows a weak reversible MAO-A and MAO-B inhibition.[19] In the literature, a modified C5 side chain (-$CONH_2$) has been reported known as the"reverse amide". The analogues containing this group have been easily obtained through total synthesis and showed a reduction in MAO inhibition and myelotoxicity, usually observed for long period treatment using Linezolid.[20] SAR studies showed that lipophilic substrates like oxazolidinones with an aromatic ring near to a nitrogen/oxygen/sulphur atom find a long and deep hydrophobic cavity. The substrates are aligned between two tyrosine residues, placing their amine near to N5 of flavin for catalysis.[21] Therefore, in the development of new oxazolidinone derivatives is essential to focus on the enhancement of antibacterial activity and on the overcoming of potential side activities of this class of molecules. Starting from all these considerations, we are searching for new analogues of Linezolid with acceptable antibacterial activity, evaluating at same time the potential effects of structural modifications on the inhibitory behaviour on MAO of these molecules (Figure 1). For this purpose, we decided to change first of all Ring-A by the introduction of i) a racemic isoster of oxazolidinone, isoxazolidinone **3**, or ii) 3,4-dehydro-β-proline **12**, we recently reported in literature as rigid five-membered heteroaromatic core for biological applications.[22] As regard isoxazolidine ring, we kept two of the three necessary features to obtain a good bioisoster of oxazolidinone: a sp^2 centre linked to Ring-B and an oxygen atom. We reported herein the synthesis of this scaffold, obtained through TBAF induced cyclization of intermediate **2 (Scheme 1)**. Two products were designed by changing the substitution on C1 of the heterocycle,[23] to evaluate if the presence of substituent in this position can influence the activity. In the case of 3,4-dehydro-β-proline containing molecules, which keep only the sp^2 centre as positive feature for interaction, worse results were expected. For both classes of compounds, as a consequence of the

synthetic route and considering the relevance that the acylaminomethyl chain has in the structure of MAO-inhibitors, we introduced a reverse N-ethyl amide without control of chirality on C5 of heterocycle, in order to understand, from a preliminary study, the potential efficacy as scaffolds of these cycles. The ring-B was linked to the heteroaromatic core through peptidic bond, keeping the fluorine atom in the usual position. Concerning the Ring-C, we used the morpholine, the piperazine or N-substituted piperazine, to evaluate if different groups may modulate the antibiotic efficacy.

2. Results and discussion

2.1. Chemistry

To substitute ring-A, two heterocycles have been used: isoxazolidin-5-one **3** and 3,4-dehydro-β-pirrole **12**. The synthesis of functionalized isoxazolidin-5-one is reported in Scheme 1. The first step of the synthesis is the 1,4-addition of *N,O*-bis(trimethylsilyl)hydroxylamine on isopropylidene and cyclohexylidene malonamides. As previously reported,[24] alkylidene malonamides react as Michael acceptors in catalytic asymmetric 1,4-addition of nitrogen nucleofiles. So, intermediates **2-a,b** have been obtained through Knövenagel condensation of the synthesized *N*-ethyl-methylmalonamide **1** with isobutyrraldehyde or cyclohexylcarboxyaldehyde in presence of a catalytic amount of piperidine, giving the product **2a** and **2b** in 55% and 56% yield respectively and 1/4 E/Z ratio. The 1,4-addition on both isomers of alkylidene malonamide was carried out through Lewis acid catalysis:[25] in dry DCM, a catalytic amount of $Sc(OTf)_3$ was added to **2** and, after lowering the temperature at -40°C, *N,O*-bis(trimethylsilyl)hydroxylamine was added. The adduct could be isolated in good yield if the temperature is mantained at -40°C, to avoid byproducts like the corresponding oxime and methylmalonamide. However, by adding TBAF in situ, it is possible to obtain at room temperature directly the product of cyclization **3-a,b** with yield of 63% and 66% respectively, through the formation of a tetrabutylammonium hydroxylamino salt that undergoes cyclization via spontaneous intramolecular transesterification. The asymmetric synthesis of 3,4-dehydro-β-pirrole **12** was achieved as reported in Scheme 1 and was already reported in previous papers.[26-27] To substitute the ring-B and ring-C, we proceeded as reported in Scheme 2. 3,4-difluorobenzoic acid was protected as methyl ester using $SOCl_2$ and methanol obtaining the intermediate **13** in 63% yield. This scaffold represents the Ring-B of the final structures. The fluorine in position 4 was used to introduce morpholine or piperazine via nucleophilic substitution reaction, with K_2HPO_4 in DMSO, obtaining intermediate **14** and **16** in 89%-99% yield. The NH moiety of piperazine was then functionalized with Boc-group in one case, obtaining intermediate **17** in quantitative yield, to avoid side reaction of this centre in subsequent reactions, and with *N*-Boc-Glycine in the other case. The coupling conditions to obtain intermediate **19** involved COMU and DIPEA and gave the desiderated intermediate in quantitative yield. The final deprotection step on intermediates **14**, **17** and **19** to remove methyl ester, was successfully performed at room temperature with $LiOH{\cdot}H_2O$ in a mixture of $THF:H_2O=2:1$, with yields between 67% and 99%. The isoxazolidin-5-one and 3,4-dehydro-β-pirrole NH derivatives **3-a,b**, **(*S*)-12** and **(*R*)-12** were coupled with the acidic counterpart **15**, **18** and **20**, in situ converted into the corresponding chloride using thionyl chloride and pyridine affording, after removal of Boc protection from intermediates, the final products **21-a,b**, **23a**, **(*S*)-24**, **(*R*)-24**, **(*S*)-26**, **(*R*)-26**, **(*S*)-28** and **(*R*)-28**. The stability of these compounds in DMSO has been verified through HPLC method and no by-products were detected in 24h study.

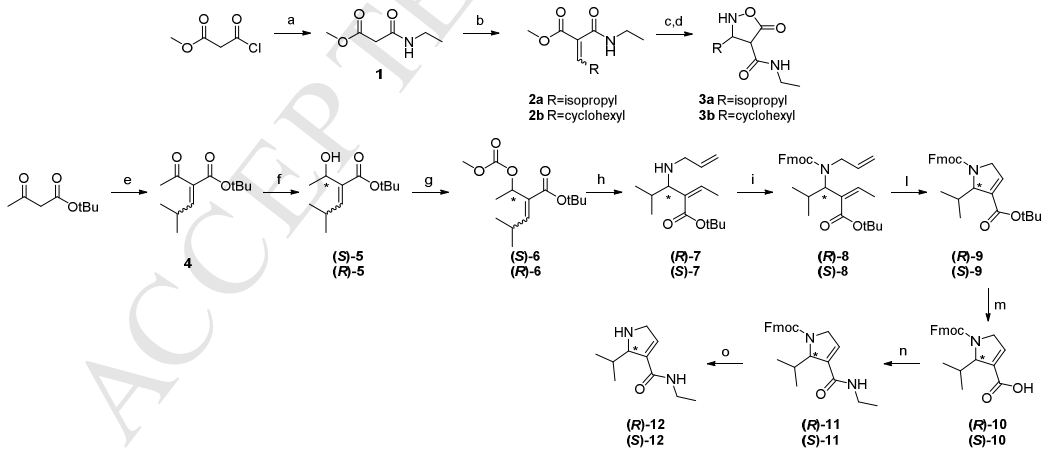

Scheme 1. Synthetic route for the synthesis of isoxazolidin-5-one ring and 3,4-dehydro-β-pirrole. Conditions: a) ethylamine, TEA, DCM, 0°C->rt, overnight; b) piperidine, aldehyde, rt, 3 days; c) $Sc(OTf)_3$, N,O-bis(trimethylsilyl)hydroxylamine, DCM, -40°C, 1.5h; d)TBAF, DCM, 15 min; e) piperidine, aldehyde, MW 250W/7 min; f) $CeCl_3.H_2O$, $NaBH_4$, THF:MeOH, -30°C, 45 min, Pseudomonas cepacia lipase, vinylacetate, Et_2O, reflux 30 h; g) LiHMDA, methylchloroformiate, THF, -78°C, 2h; h) $[Ir(COD)Cl]_2$, $P(OPh_3)$, allylamine, EtOH, 24h; i) $NaHCO_3$, Fmoc-Cl, dioxane, rt, overnight ; l) MTBE, Grubbs-II generation catalyst, 50°C, 20h; m) TFA, 0°C->rt, overnight; n) ethylamine, HBTU, TEA, DCM, rt, overnight; o) piperidine, DMF, rt, 10 min.

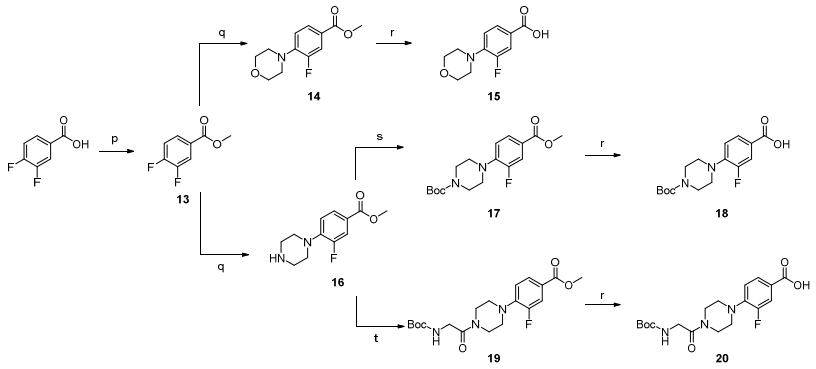

Scheme 2. Synthetic route for the synthesis of Ring-B and Ring-C. Conditions: p) $SOCl_2$, MeOH, 0°C->rt, overnight; q) morpholine/piperazine, K_2HPO_4, dmso, reflux, 8h; r) LiOH·H_2O, THF:H_2O, rt, overnight.

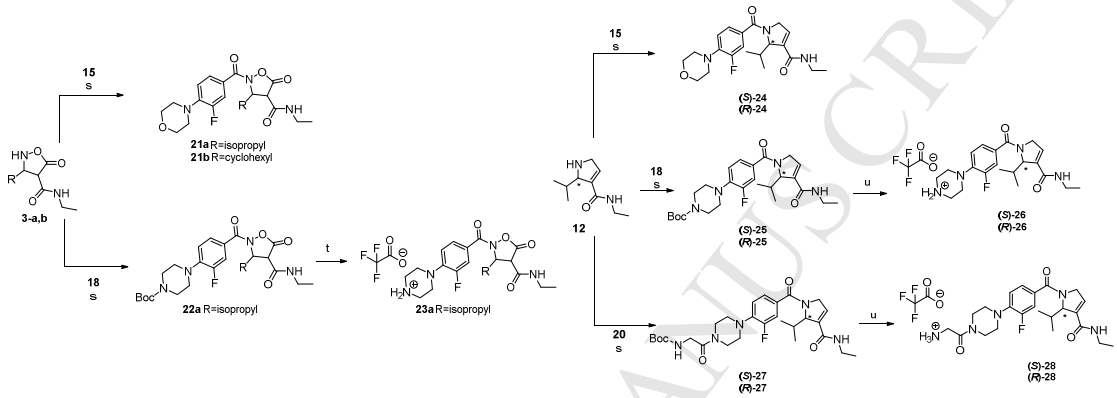

Scheme 3. Synthesis of isoxazolidin-5-one and 3,4-dehydro-β-pirrole derivatives.

	MIC (μg/ml)		MIC-range	MIC_{50}	MIC_{90}
Strains	*S. aureus* ATCC 29213	*E. faecalis* ATCC 29212	12 *S. aureus* isolates		
Compound					
21a	**>128**	**>128**	**>128**	**>128**	**>128**
21b	**>128**	**>128**	**32->128**	**64**	**>128**
(*R*)-24	**>128**	**>128**	**>128**	**>128**	**>128**
(*S*)-24	**>128**	**>128**	**>128**	**>128**	**>128**
Linezolid	**4**	**2**	**1-4**	**2**	**2**

Table 1. Antimicrobial activities, expressed in MIC values, MIC-range, MIC_{50} and MIC_{90} (μg/ml) of tested compounds against both Gram-positive standard strains and recently isolated clinical *Staphylococcus aureus* strains; Linezolid was used as reference antibiotic agent.

2.2 Biological evaluation

The antibacterial activity of all the synthesized products **21-a,b**, **23a**, **(*S*)-24**, **(*R*)-24**, **(*S*)-26**, **(*R*)-26**, **(*S*)-28** and **(*R*)-28** was evaluated on MRSA and MSSA strains, but after the initial unsatisfactory results, only the activities of **21a**, **21b**, **24- (R)** and **24-(S)** compounds were further explored.

The antibacterial activities of **21a**, **21b**, **(*R*)-24** and **(*S*)-24** by means of MIC values are shown in Table 1. Only for **21b** a modest antibacterial activity (MIC=32-64 μg/ml) against clinical strains of *S. aureus* was demonstrated.

Therefore, **21a**, **21b**, **(*R*)-24** and **(*S*)-24** compounds are weak antibiotics with respect to Linezolid (LZD); nevertheless, they might be better utilized as MAO inhibitors. For this reason their potential MAO activity inhibitory power was analyzed along with their cytotoxicity in an in vitro system, that, is an excellent model to perform preliminary screening. HepG2 cells, derived from human hepatocytoma, were chosen in this study since both MAO-A and -B have been found in human liver tissue and in hepatocytes as well and because of this cell line is easy to maintain and proliferate rapidly.[28-29]

Cell viability experiments were performed to define the proper dose for the evaluation of compounds effects on MAO activity in HepG2, taking into account the previous data obtained with Linezolid,[30] used as oxazolidinones reference drug.

Increasing concentrations (10-100μg/mL) of **21a**, **21b**, **(*R*)-24** and **(*S*)-24** were administrated to cells for 24 hours. None of compounds treatments induces mortality at 10μg/mL, while at ten-times increasing concentration we observed only a 10% decrease in cell viability with **21a**, **21b**, **(*R*)-24** and 20% in **(*S*)-24**. Since **21a**, **21b**, **(*R*)-24** and **(*S*)-24** compounds are all dissolved in DMSO, the effect of **(*S*)-24** on cell viability is probably due to the cytotoxicity exerted by high percentage of solvent (2%) in which it is solubilized (data not shown).

MAO activity was analyzed in HepG2 cell lysates after 24 hours of treatment with 10-100μg/mL of **21a**, **21b**, **(*R*)-24** and **(*S*)-24** compounds, using the Amplex® Red Monoamine Oxidase assay. The **21a**, **21b** and **(*S*)-24** compounds showed a significative inhibitory effect of about 25% already at 10μg/mL. Thus, considering the mild cytotoxicity exerted in HepG2, we increased ten-times the drug concentration reaching the 45% of inhibitory effect. On the contrary, high concentration (100μg/mL) of Linezolid (LZD) induces a weak decrease of enzymatic activity (15%). In agreement to our data, experimental evidences demonstrated a low inhibitory effect of LZD on MAO activity in a cell-free assay.[12]

Taken together, cell viability and MAO activity assays showed that **21a**, **21b** and **(*S*)-24** molecules might be promising compounds for the development of MAO inhibitors, showing a very low cytotoxicity also at the concentration exerting almost 50% of inhibitory effect. Nevertheless, our compounds deserve future experiments to confirm their potential inhibitory efficacy, analyzing also their specificity for MAO-A or MAO-B.

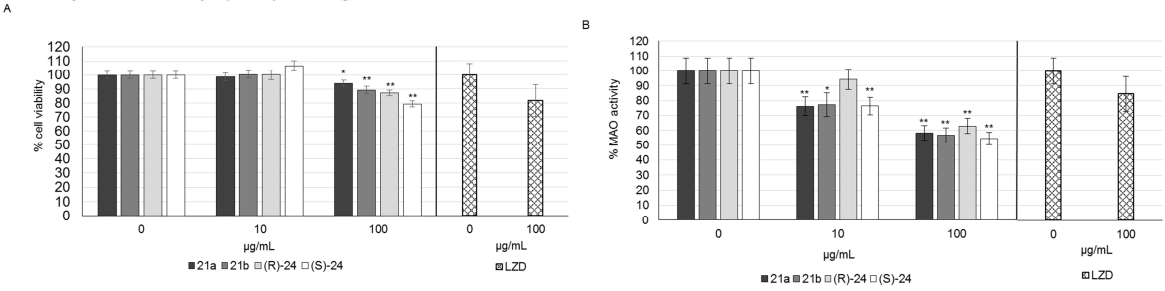

Figure 3. A) Cell viability of 21a, 21b, (*R*)-24, (*S*)-24 and Linezolid in HepG2 cells. B) MAO activity of 21a, 21b, (*R*)-24, (*S*)-24 and Linezolid in HepG2 cells.

2.3 Structure-activity relationships

In this work we reported how the substitution of oxazolidinone ring with isoxazolidinone or 3,4-dehydro-β-proline led to a loss of antibacterial activity against the bacterial strains previously reported. By the prediction of log P_{Kow} calculated through EPI Suite™ for each compound and for the reference compound Linezolid, we found a rational trend. All the compounds containing isoxazolidinone ring have an hydrophilic behaviour while those containing 3,4-dehydro-β-proline belong to the family of lipophilic compounds. In the first family, while the isopropyl group does not affect the hydrophilicity, the cyclohexyl group induces an enhancement of log *P* meaning a more lipophilic behaviour. Regarding the second family, modulation of lipophilicity depends on the Ring C: going from morpholine to Gly-piperazine through piperazine, the log P value is mitigated toward more hydrophilic character. As shown in Table 2, the compound **21b** has log *P* value quite near to that of Linezolid, confirming that the changes in terms of hydrophilicity/lipophilicity affect considerably the interaction of these compounds with the binding site.

Compound	log P_{Kow}
21a	-0.26
21b	1.10
23a*	-0.50
(S)-24	1.72
(S)-26	1.48
(S)-28	0.10
Linezolid	1.26

Table 2. Prediction of log P_{Kow}. *(*the log P was calculated for the neutral form of this compound)*

2.4 Modeling studies

To get some insight into the binding modes of the newly prepared compounds, we performed a docking study into the active site of human monoamine oxidase isoforms A (MAO-A) and B (MAO-B). The crystal structures of MAO-A[31] and MAO-B[32] were retrieved from the Protein Data Bank (PDB codes: 2Z5X[33] and 2V5Z,[34] respectively) and processed using Schrödinger Protein Preparation Wizard.[35] A small library of compounds was built including all the four possible stereoisomers of isoxazolidinones **21a** and **21b** (**(*R,R*)-21a,b**, **(*R,S*)-21a,b**, **(*S,R*)-21a,b**, **(*S,S*)-21a,b**), the two enantiomers of the 3,4-dehydro-β-pirrole derivative **24** (**(*R*)-24** and **(*S*)-24**) and (*S*)-Linezolid as a reference ligand. The library of compounds was optimized by molecular mechanic and docking was performed with AutoDock Vina.[36]

The binding free energies calculated for the human MAO-A model were invariably much lower for all compounds examined, with respect to the reference ligand (*S*)-Linezolid and only compounds **(*S*)-24**, **(*R*)-24**, **(*R,R*)-21a** and **(*R,R*)-21b** displayed negative binding free-energy values (Table 3).

Compound	Free energy of binding (kcal/mol)
S-Linezolid	-6.2
***S*-24**	-2.0
***RR*-21b**	-1.7
***RR*-21a**	-0.3
***R*-24**	-0.2

Table 3. Docking scores (MAO-A) for compounds **24**, (*R,R*)-**21a-b**, and (*S*)-Linezolid.

Both (*S*)-Linezolid and **(*S*)-24** direct the morpholine ring (ring-C) toward the MAO-A aromatic cage, formed by FAD, TYR-407 and TYR-444. On the other side, **(*S*)-24** is forced to penetrate deeper into the binding site of MAO-A in order to accommodate the bulky isopropyl group in the same space occupied by the oxazolidinone ring (ring-A) of (*S*)-Linezolid (Figure 4). A single hydrogen bond interaction was found for the tail amide NH bond of (*S*)-Linezolid with VAL-210, as well as for the central C=O bond of **(*S*)-24** with THR-336.

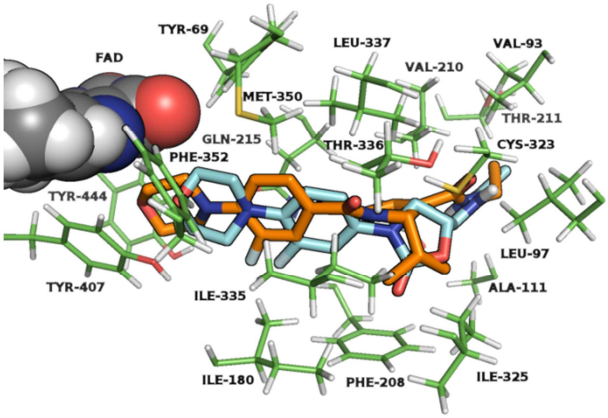

Figure 4. Best docking pose of (*S*)-Linezolid (cyan carbon atoms) superimposed to the best docking pose of (*S*)-24 (orange carbon atoms) in the active site of MAO-A. Residues of the binding site are represented with green carbon atoms and FAD as CPK.

A similar binding pose was found also for the enantiomeric compound **(*R*)-24**, which is forced even deeper into the MAO-A aromatic cage due to the different spatial disposition of the isopropyl substituent (Figure 5). Also in this case, a single hydrogen bond interaction was found for the tail amide NH bond of **(*R*)-24** with PHE-208.

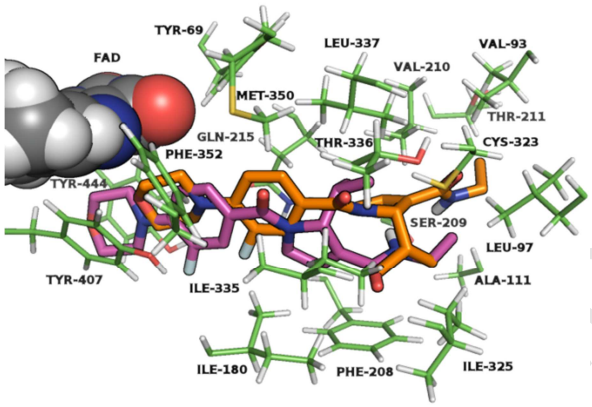

Figure 5. Best docking pose of (*S*)-24 (orange carbon atoms) superimposed to the best docking pose of (*R*)-24 (purple carbon atoms) in the active site of MAO-A. Residues of the binding site are represented with green carbon atoms and FAD as CPK.

Interestingly, isoxazolidinones **(*R,R*)-21a** and **b** displayed two almost superimposable docking poses, completely different to the one of the reference ligand (*S*)-Linezolid (Figure 6). The *N*-ethyl amide tail of the two isoxazolidinones is in this case directed toward the aromatic cage of MAO-A, whereas the morpholine ring (ring-C) is positioned in the direction of the cavity entrance, in the pocket formed by VAL-93, LEU-97 and THR-211.

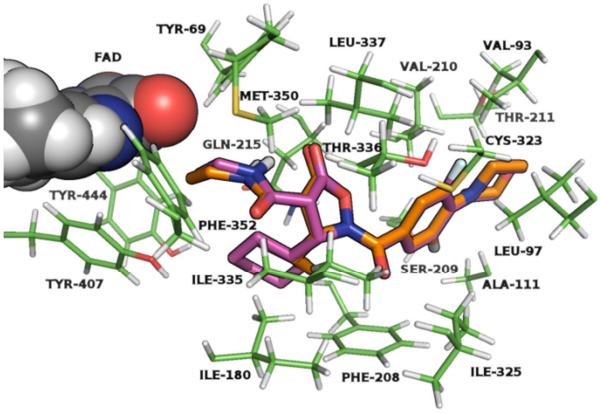

Figure 6. Best docking pose of (*R,R*)-21a (orange carbon atoms) superimposed to the best docking pose of (*R,R*)-21b (purple carbon atoms) in the active site of MAO-A. Residues of the binding site are represented with green carbon atoms and FAD as CPK.

Much better and encouraging results were found in the docking of compounds **21a**, **21b** and **24** to the human MAO-B model, as evidenced by the best calculated binding free energies reported in Table 4. For all compound examined, a second almost isoenergetic binding pose was invariably found, differing only in the relative disposition of the fluorinated aromatic ring (ring-B). Moreover, for all compounds with the exception of **(*R,R*)-21b**, two distinct binding poses with very similar energies were located. They differ for the relative orientation of the ligand in the binding site, one (**A**) having the morpholine ring (ring-C) and the other (**B**) having the amide tail directed toward the MAO-B aromatic cage, formed by TYR-398 and TYR-435.

Compound	Free energy of binding (kcal/mol)
R-**24**	-8.4 (**A**), -8.9 (**B**)
S-Linezolid	-7.4 (**A**), -7.6 (**B**)
RR-**21a**	-7.2 (**A**), -6.8 (**B**),
SR-**21a**	-6.5 (**A**), -6.7 (**B**)
RR-**21b**	-4.5 (**A**),
S-**24**	-4.1 (**A**), -3.6 (**B**),

Table 4. Docking scores (MAO-B) for compounds **24**, (*R,R*)-**21a-b**, and (*S*)-Linezolid.

The morpholine ring (ring-C) and the aromatic ring (ring-B) of the best docking poses of **(*R*)-24** and of (*S*)-Linezolid are almost perfectly superimposed, confined in the bounding region between the entrance cavity and the substrate cavity defined by ILE-199. Accordingly, the amide tails are directed toward the aromatic cage of MAO-B, between TYR-398 and TYR-435 (Figure 7). A network of four hydrogen bonds contributes to stabilize the docking pose of **(*R*)-24**, namely between the tail NH bond and GLN-206, the tail amide C=O bond and both TYR-435 and CYS-172 and the central amide C=O bond and TYR-326. Two relevant hydrogen bond interactions were found for (*S*)-Linezolid, one between the tail NH bond and TYR-398 and the other between the oxazolidinone C=O bond and ILE-198.

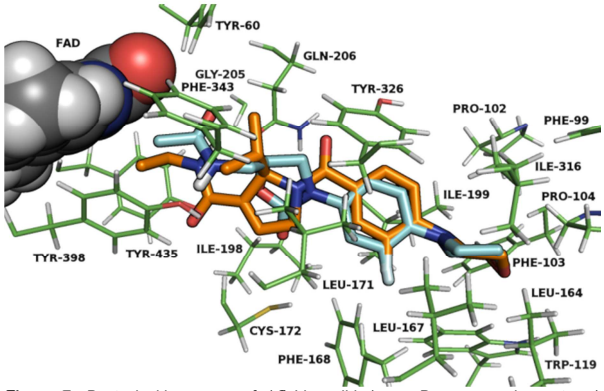

Figure 7. Best docking pose of (*S*)-Linezolid (pose B, cyan carbon atoms) superimposed to the best docking pose of (*R*)-24 (pose B, orange carbon atoms) in the active site of MAO-B. Residues of the binding site are represented with green carbon atoms and FAD as CPK.

As mentioned previously, the best docking pose for the 3,4-dehydro-β-pirrole derivative **(*S*)-24** is oriented differently with respect to its enantiomer **(*R*)-24**, directing the morpholine ring (ring-C) toward the aromatic cage of MAO-B and the amide tail

in the direction of the entrance cavity (Figure 8). A single hydrogen bond interaction was found for **(*S*)-24**, involving the central amide C=O bond and ILE-199.

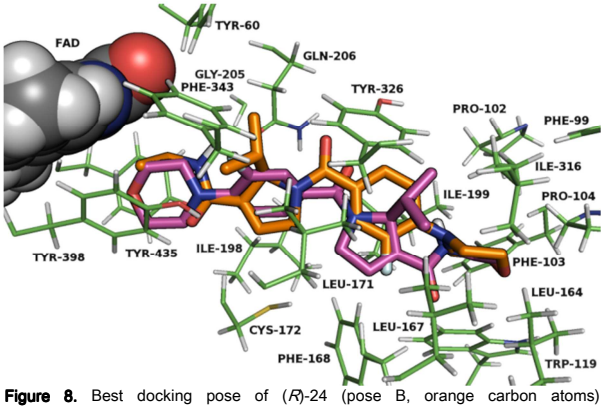

Figure 8. Best docking pose of (*R*)-24 (pose B, orange carbon atoms) superimposed to the best docking pose of (*S*)-24 (pose A, purple carbon atoms) in the active site of MAO-B. Residues of the binding site are represented with green carbon atoms and FAD as CPK.

The possible binding poses (**A** and **B**) for isoxazolidinones **(*R,R*)-21a** and **(*S,R*)-21a**, differing only in the configuration of the isopropyl substituted carbon, are reported in Figures 9 and 10, respectively. Three relevant hydrogen bond interactions are present in both poses of **(*R,R*)-21a**. In pose A they involve the isoxazolidone carbonyl with TYR-326 and ILE-199 and the tail amide C=O bond with PRO-102, while in pose B the hydrogen bonds are formed between the tail NH bond and GLN-206, the tail amide C=O bond and LEU-171 and the central amide C=O bond and TYR-326.

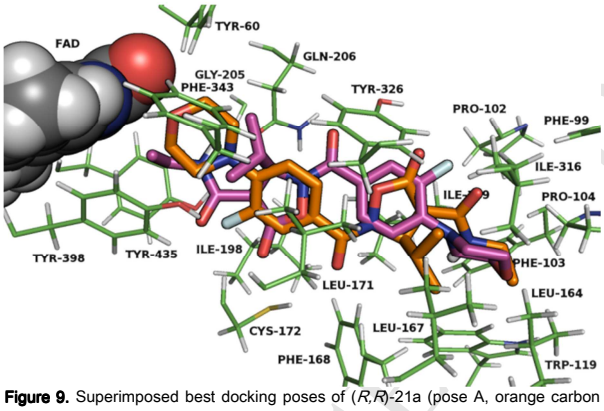

Figure 9. Superimposed best docking poses of (*R,R*)-21a (pose A, orange carbon atoms) and pose B, purple carbon atoms) in the active site of MAO-B. Residues of the binding site are represented with green carbon atoms and FAD as CPK.

In the case of **(*S,R*)-21a**, two hydrogen bond interactions were found only for pose A, involving the central amide C=O bond and TYR-326 and the isoxazolidone carbonyl group with PHE-168.

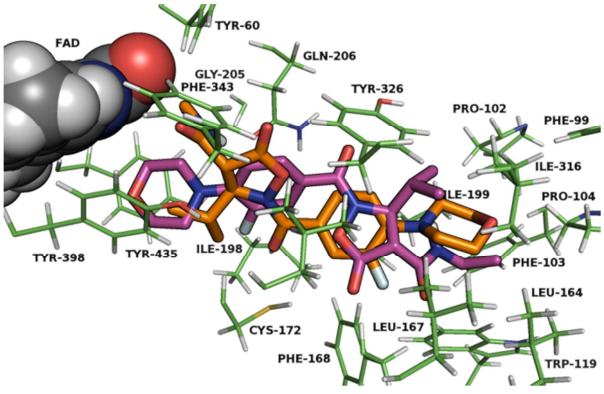

Figure 10. Superimposed best docking poses of (*S,R*)-21a (pose B, orange carbon atoms) and pose A, purple carbon atoms) in the active site of MAO-B. Residues of the binding site are represented with green carbon atoms and FAD as CPK.

Finally, the only suitable docking pose for the hindered cyclohexyl-substituted isoxazolidinone ***(R,R)*-21b** is reported in Figure 11, superimposed to best docking pose of the isopropyl-substituted analogue **(*R,R*)-21a**. Again, as we found for the docking poses involving MAO-A, the two poses are almost perfectly superimposed, with the bulky cyclohexyl substituent confined in the region delimited by LEU-167, ILE-316 and LEU-164.

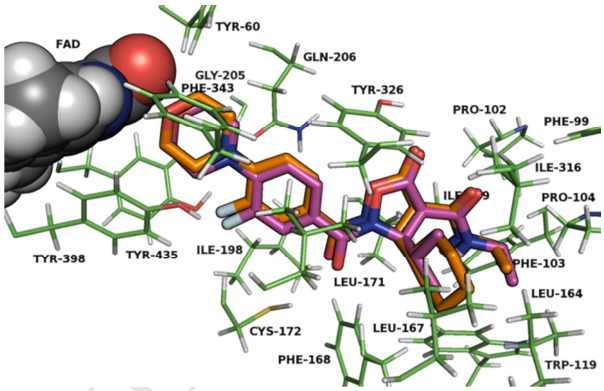

Figure 11. Best docking pose of (*R,R*)-21b (orange carbon atoms) superimposed to the best docking pose of (*R,R*)-21a (pose A, purple carbon atoms) in the active site of MAO-B. Residues of the binding site are represented with green carbon atoms and FAD as CPK.

Not surprisingly, possessing almost an identical orientation in the binding site of MAO-B, the same network of hydrogen bonds characterizing **(*R,R*)-21a** between the isoxazolidinone carbonyl with TYR-326 and ILE-199 and the tail amide C=O bond with PRO-102, was found also for **(*R,R*)-21b** .

Modeling studies seem to suggest that all the members of the new family of compounds synthesized are selective against the binding to MAO-B receptor. In particular the 3,4-dehydro-β-pirrole derivative **(*R*)-24** seems the more promising, displaying an affinity for the binding site of MAO-B similar or even greater to that of the reference ligand (*S*)-Linezolid. Moreover, it is worth to note that also its enantiomer **(*S*)-24** seems to display a good degree of selectivity against MAO-B receptor. Among the family of isopropyl-substituted isoxazolidinones **21a**, only the ones possessing the *R* configuration at the C4 stereocenter, namely **(*R,R*)-21a** and **(*S,R*)-21a**, displayed favourable binding energies to MAO-B receptor. Interestingly, the absolute orientation of the substituent in C4 for these two compounds is the same of the acetamido-methyl substituent on the oxazolidinone ring of (*S*)-Linezolid. Finally, among the more hindered isoxazolidone analogues **21b**, only the *RR*-stereoisomer displayed a moderate activity against MAO-B isoform. For all the other stereoisomers, no suitable low energy binding poses were found, due to the steric clashes invariably present between the bulky cyclohexyl substituent and the residues of the binding site.

3. Conclusion

The balance between antibiotic activity and MAO-inhibition is an important issue to be considered when developing oxazolidinone based bioactive compounds. In this work we reported novel compounds, designed to be Linezolid analogues, where isoxazolidinone or 3,4-dehydro-β-proline were introduced as scaffolds in substitution of

oxazolidinone ring. Among the small library of synthesized compounds, only one showed a modest antibiotic effect, thus demonstrating that the changes in the molecule backbone were detrimental for antibacterial activity. On the other hand, a promising inhibitory effect on to monoamino oxidase (MAO) was observed and confirmed by docking experiments that suggested a good interaction of all the members of the new family of compounds on MAO-B receptor. In particular the 3,4-dehydro-β-pirrole derivative (*R*)-**24** seems the more promising, displaying an affinity for the binding site of MAO-B.

4. Experimental

4.1. Chemistry

All chemicals were purchased from commercial suppliers and used without further purification. Anhydrous solvents were purchased in sure seal bottles over molecular sieves and used without further drying. Flash chromatography was performed on silica gel (230–400 mesh). NMR Spectra were recorded with Mercury Plus 400 MHz spectrometers. Chemical shifts were reported as δ values (ppm) relative to the solvent peak of $CDCl_3$ set at δ= 7.27 ppm (^{1}H-NMR) or δ = 77.0 ppm (^{13}C-NMR), CD_3OD set at δ = 3.31 ppm (^{1}H-NMR) or δ = 49.0 ppm (^{13}C-NMR), D_2O set at δ = 4.79 ppm (^{1}H-NMR). Coupling constants are given in Hertz. Optical rotations were measured in a Perkin Elmer 343 polarimeter using a 1 dm cuvette and are referenced to the Na-D line value. LC–MS analyses were performed on a HP1100 liquid chromatography coupled with an electrospray ionization-mass spectrometer (LC–ESI–MS), using H_2O/CH3CN or H_2O/CH_3CN acid for 0.2% of CH_2O_2 as solvents at 25° C (positive scan 100–500 m/z, fragmentor 70 V).

4.2. Synthesis

(1)

In a 2-necked round-bottom flask, equipped to perform reaction under N_2, ethylamine (1.2 eq, 22.3 mmol) and TEA (2 eq, 37.2 mmol) were added in dry DCM (19 ml). Methyl malonyl chloride (1 eq, 18.6 mmol) was added dropwise at 0°C and the mixture stirred at room temperature overnight. The reaction was quenched with water and the product extracted with DCM. The product was used without further purifications (Y%>99%).

(**1**): Pale yellow oil; ^{1}H-NMR (400 MHz, $CDCl_3$) δ 7.02 (bs, 1H), 3.73 (s, 3H), 3.44-3.27 (m, 2H), 3.29 (s, 2H), 1.14 (dt, ^{3}J=7.2 Hz, ^{4}J=1.6 Hz, 3H). ^{13}C-NMR (400 MHz, $CDCl_3$) δ168.2, 166.4, 51.1, 36.5, 33.7, 14.9. LC-ESI-MS: 1.5 min, $[M+H]^+$=146, $[M+Na]^+$=178, $[2M+Na]^+$=313.

(2a), (2b)

Compound **1** (1 eq, 8.97 mmol), piperidine (0,15 eq, 1.35 mmol) and aldehyde (1.7 eq, 15.2 mmol) were stirred at room temperature for 3 days. The crude was poured in water and extracted with EtOAc. Purification by flash chromatography (silica gel, 9:1=Cy:EtOAc) allowed to isolate the product as a mixture of two isomers (Z/E=4/1).

Yield of (**2a**): 55%. Yield of (**2b**): 56%.

(2a) *E*-isomer: Yellow oil; ^{1}H-NMR (400 MHz, $CDCl_3$) δ 6.90 (d, ^{3}J=10.4 Hz, 1H), 6.88 (bs, 1H), 3.76 (s, 3H), 3.40-3.34 (m, 2H), 3.26 (m, 1H), 1.18 (t, ^{3}J=7.2 Hz, 3H), 1.06 (d, ^{3}J=6.8 Hz, 6H). ^{13}C-NMR (400 MHz, $CDCl_3$) δ166.5, 162.1, 160.3, 124.5, 51.2 , 43.5, 29.1, 21.8, 14.9. LC-ESI-MS: 8.8 min $[M+H]^+$=200, $[M+K]^+$=238, $[2M+Na]^+$=421 **Z-isomer:** Yellow oil; ^{1}H-NMR (400 MHz, $CDCl_3$) δ 6.88 (bs, 1H), 6.79 (d, ^{3}J=10.4 Hz, 1H), 3.76 (s, 3H), 3.40-3.34 (m, 2H), 3.26 (m, 1H), 1.18 (t, ^{3}J=7.2 Hz, 3H), 1.06 (d, ^{3}J=6.8 Hz, 6H).^{13}C-NMR (400 MHz, $CDCl_3$) δ167.7, 163.3, 160.3, 125.0, 51.3, 43.3, 28.9, 21.8, 14.9. LC-ESI-MS: 8.0 min $[M+H]^+$=200, $[M+K]^+$=238, $[2M+Na]^+$=421.

(2b) *E*-isomer: Yellow oil;^{1}H-NMR (400 MHz, $CDCl_3$) δ 6.91 (d, ^{3}J=10.4 Hz, 1H), 6.93 (bs, 1H), 3.74 (s, 3H), 3.41-3.30 (m, 2H), 3.75 (m, 1H), 1.73-1.64 (m, 5H), 1.37-1.07 (m, 5H), 1.17 (t, ^{3}J=7.2 Hz, 3H). ^{13}C-NMR (400 MHz, $CDCl_3$) δ164.3, 163.7, 155.3, 125.6, 51.3, 38.0, 33.7, 31.3, 25.2, 24.7, 14.0. LC-ESI-MS: 8.9 min, $[M+H]^+$=240, $[M+Na]^+$=262, $[2M+Na]^+$=501. **Z-isomer:** Yellow oil; ^{1}H-NMR (400 MHz, $CDCl_3$) δ 6.80 (d, ^{3}J=10.4 Hz, 1H), 6.93 (bs, 1H), 3.74 (s, 3H), 3.41-3.30 (m, 2H), 3.75 (m, 1H), 1.73-1.64 (m, 5H), 1.37-1.07 (m, 5H), 1.17 (t, ^{3}J=7.2 Hz, 3H). ^{13}C-NMR (400 MHz, $CDCl_3$) δ166.7, 164.1, 155.3, 126.8, 51.5, 38.0, 33.7, 31.3, 25.2, 24.7, 14.0. LC-ESI-MS: 6.6 min $[M+H]^+$=240, $[M+Na]^+$=262, $[2M+Na]^+$=501.

(3a), (3b)

In a 2-necked round-bottom flask, equipped to perform reaction under N_2 flow, **2** (1 eq, 3.44 mmol) was dissolved in dry DCM (17.2 ml) togheter with $Sc(OTf)_2$ and stirred at room temperature for 15 min. The mixture was cooled to -40 °C and N,O-bis(trimethylsilyl) hydroxylamine (1.5 eq, 5.16 mmol) was added. After stirring for 1.5 h, Tetrabutylammonium fluoride (2 eq, 6.88 mmol) was added and the mixture stirred at room temperature for further 15 min. The reaction was quenched with water and the crude extracted with DCM. Purification was pefomed by flash chromatography (silica gel, 8:2->7:3=Cy:EtOAc).

Yield of (**3a**): 63%. Yield of (**3b**): 66%.

(3a): Waxy solid ^{1}H-NMR (400 MHz, $CDCl_3$) δ 6.34 (bs, 1H), 3.94 (dd, ^{3}J=6.4 Hz, ^{3}J=4.4 Hz, 1H), 3.39-3.26 (m, 2H), 3.30 (d, ^{3}J=6.4 Hz, 1H), 1.91 (m, 1H), 1.16 (t, ^{3}J=7.2 Hz, 3H), 0.99 (d, ^{3}J=6.8 Hz, 3H), 0.97 (d, ^{3}J=6.8 Hz, 3H). ^{13}C-NMR (400 MHz, $CDCl_3$) δ165.9, 163.9, 66.5, 51.4, 35.1, 30.8, 18.9 18.0, 14.4. LC-ESI-MS: 2.4 min, $[M+H]^+$=201, $[M+Na]^+$=223, $[M+K]^+$=239.

(3b): Waxy solid ^{1}H-NMR (400 MHz, $CDCl_3$) δ 6.27 (bs, 1H), 3.97 (dd, ^{3}J=6.4 Hz, ^{3}J=5.6 Hz, 1H), 3.38-3.27 (m, 2H), 3.31 (d, ^{3}J=5.2 Hz, 1H), 1.84-1.55 (m, 6H), 1.27-1.02 (m, 5H), 1.16 (t, ^{3}J=7.2 Hz, 3H). ^{13}C-NMR (400 MHz, $CDCl_3$) δ165.5, 163. 5, 66.9, 51.9, 40.1, 34.7, 28.9, 26.5, 25.7, 25.4, 25.3, 13.9. LC-ESI-MS: 5.8 min, $[M+H]^+$=241, $[M+Na]^+$=263, $[M+K]^+$=279.

(4)

Mono-tertbutyl acetoacetate (1 eq, 24.14 mmol), isobutyraldheyde (1.7 eq, 41.03 mmol) and piperidine (0.15 eq, 3.62 mmol) were mixed and irradiated using microwaves at 250 watt for 7 min. The reaction was quenched with water and the crude extracted with EtOAc. The product was isolated (Y%=64%, E/Z=1/4) by flash chromatography (silica gel, 95:5=Cy:EtOAc).

***E*-isomer:** Pale yellow oil ^{1}H-NMR (400 MHz, $CDCl_3$) δ6.58 (d, ^{3}J=10.6 Hz, 1H), 2.60 (m, 1H), 2.34 (s, 3H), 1.55 (s, 9H), 1.09 (d, ^{3}J=6.6 Hz, 6H). ^{13}C-NMR (400 MHz, $CDCl_3$)δ197.3, 165.4, 154.2, 132.9, 79.8, 29.4, 28.7, 24.2, 22.0. LC-ESI-MS: 10.1 min, $[M+Na]^+$=235, $[2M+Na]^+$=467. **Z-isomer:** Pale yellow oil ^{1}H-NMR (400 MHz, $CDCl_3$) δ6.53 (d, ^{3}J=10.6 Hz, 1H), 2.65 (m, 1H), 2.30 (s, 3H), 1.51 (s, 9H), 1.45 (d, ^{3}J=6.6 Hz, 6H). ^{13}C-NMR (400 MHz, $CDCl_3$)δ197.3, 165.4, 154.2, 132.9, 79.8,

29.6, 28.7, 24.4, 21.9. LC-ESI-MS: 9.3 min $[M+Na]^+$=235, $[2M+Na]^+$=467.

*(**5**)*

In a 2-necked round-bottom flask, equipped to perform reaction under N_2 flow, *Z*-**4** (1 eq, 8.25 mmol) was dissolved in a mixture of THF:MeOH=9:1 (82.5 ml) and $CeCl_3.H_2O$ (1 eq, 8.25 mmol) was added. The mixture was stirred at room temperature for 30 min, then it was cooled at -30 °C and $NaBH_4$ (1.1 eq, 9.08 mmol) was added. After 45 min of stirring at -30 °C, the reaction was quenched with water and the crude extracted with EtOAc. Purification by flash chromatography (silica gel, 95:5=Cy:EtOAc) allowed to isolate the product (Y%=92%). Racemic **5** was then dissolved in Et_2O (42.5 ml), and vinylacetate (5 eq, 37.9 mmol) and Pseudomonas cepacia lipase (35 mg/ml) were added. The mixture was refluxed for 30 h and then filtered to recover the enzyme. The organic phase was concentrated and the crude was purified by flash chromatography (silica gel, 95:5=Cy:EtOAc) to isolate the product **(S)-5** and the corresponding acetate of the R enantiomer, that was hydrolysed with K_2CO_3 (1 eq) in MeOH by stirring the mixture for 30 min at room temperature, and then quenching it with HCl 1M. The product **(R)-5** obtained from extraction with EtOAc was used without further purifications.

Yield of **(*S*)-5**: 94%. Yield of **(*R*)-5**: 90%.

***E*-isomer:** Yellow oil; ^{1}H-NMR (400 MHz, $CDCl_3$) δ6.37(d, ^{3}J=10.4 Hz, 1H), 4.10 (q, ^{3}J=6.8 Hz, 1H), 3.03 (m, 1H), 1.51 (s, 9H), 1.32 (d, ^{3}J=6.6 Hz, 3H), 0.99 (d, ^{3}J=8 Hz, 6H). ^{13}C-NMR (400 MHz, $CDCl_3$) δ166.8, 147.3, 131.9, 81.0, 58.6, 29.1, 28.3, 22.6, 22.4. ***Z*-isomer:** Yellow oil; ^{1}H-NMR (400 MHz, $CDCl_3$) δ5.75 (d, ^{3}J=10 Hz, 1H), 4.36 (q, ^{3}J=6.4 Hz, 1H), 3.03 (m, 1H), 1.51 (s, 9H), 1.32 (d, ^{3}J=6.6 Hz, 3H), 0.99 (d, ^{3}J=8 Hz, 6H). ^{13}C-NMR (400 MHz, $CDCl_3$) δ167.2, 146.7, 130.1, 81.1, 58.8, 28.2, 27.7, 22.6, 22.4. LC-MS (ESI): 1.6 min, $[M+H]^+$=215, $[M+Na]^+$=227, $[2M+Na]^+$=451. *S*-enantiomer $[\alpha]_D$= -26, *R*-enantiomer $[\alpha]_D$= +38 (*c* 1 in $CHCl_3$).

*(**6**)*

In a 2-necked round bottom flask, equipped to perform reaction under N_2 flow, each enantiomer of *Z*-**5** (1 eq, 1.83 mmol) was dissolved in THF at -78 °C. LiHMDA (1.5 eq, 2.74 mmol) was added and the mixture was stirred for 30 min. Methyl chloroformiate (2 eq, 3.66 mmol) was added dropwise and the mixture was stirred for 1.5 h at -78 °C. The reaction was quenched with water and the crude extracted with EtOAc. It was purified by flash chromatography (silica gel, 95:5=Cy:EtOAc) to isolate the product .

Yield of **(*S*)-6**: 75%. Yield of **(*R*)-6**: 78%.

***E*-isomer:** Transparent oil; ^{1}H-NMR (400 MHz, $CDCl_3$) δ5.81 (dd, ^{3}J=9.6 Hz, ^{4}J=1.2 Hz, 1H), 5.44 (q, ^{3}J=6.4 Hz, 1H), 3.77 (s, 3H), 3.15 (m, 1H), 1.51 (s, 9H), 1.40 (d, ^{3}J=6.8 Hz, 3H), 0.99 (d, ^{3}J=6.8 Hz, 6H). ^{13}C-NMR (400 MHz, $CDCl_3$) δ165.6, 155.0, 146.7, 131.3, 81.2, 74.0, 54.5, 28.1, 26.2, 22.5, 19.8. LC-ESI-MS: 11.8 min $[M+H]^+$=273, $[M+Na]^+$=295. ***Z*-isomer :** Transparent oil; ^{1}H-NMR (400 MHz, $CDCl_3$) δ5.76 (d, ^{3}J=9.6 Hz, 1H), 4.36 (q, ^{3}J=6.4 Hz, 1H), 3.77 (s, 3H), 3.00 (m, 1H), 1.48 (s, 9H), 1.32 (d, ^{3}J=6.4 Hz, 3H), 0.99 (d, ^{3}J=6.8 Hz, 6H). ^{13}C-NMR (400 MHz, $CDCl_3$) δ165.6, 155.0, 146.7, 131.3, 81.2, 74.0, 54.5, 28.1, 26.2, 22.5, 19.8. LC-ESI-MS: 8.9 min, $[M+H]^+$=273, $[M+Na]^+$=295. *S*-enantiomer $[\alpha]_D$= -30.0, *R*-enantiomer $[\alpha]_D$= +28.9 (*c* 1 in $CHCl_3$).

*(**7**)*

In a 2-necked round bottom flask, equipped to perform reaction under N_2 flow, $[Ir(COD)Cl]_2$ (0.02 eq, 0.03 mmol) and $P(OPh)_3$ (0.08 eq, 0.13 mmol) were dissolved in dry EtOH (8.25 ml) and the mixture stirred for 20 min. Allylamine (1 eq, 1.65 mmol) was added and the mixture was stirred for 20 min. Then **6** (1 eq, 1.65 mmol) and another aliquot of allylamine (4 eq, 6.6 mmol) were added and the mixture refluxed for 24 h. The reaction was quenched with water and the crude was extracted with EtOAc. After removal of the solvent under vacuum, the crude was used in the next step without further purifications.

*(**8**)*

*(**7**):* Sticky solid; ^{1}H-NMR (400 MHz, $CDCl_3$) δ6.89 (q, ^{3}J= 7.2 Hz, 1H), 5.86 (m, 1H), 5.15 (dd, ^{3}J=17.2 Hz, ^{2}J=2 Hz, 1H), 5.03 (dd, ^{3}J=10.4 Hz, ^{2}J=1.6 Hz, 1H) 3.22 (dd, ^{3}J=14 Hz, ^{3}J=5.2 Hz, 1H), 3.08 (d, ^{3}J=9.2 Hz, 1H), 2.96 (dd, ^{2}J=14 Hz, ^{3}J=6.8 Hz, 1H), 1.92 (m, 1H), 1.75 (d, ^{3}J=7.2 Hz, 3H), 1.46 (s, 9H), 1.07 (d, ^{3}J=6.4 Hz, 3H), 0.74 (d, ^{3}J=6.4 Hz, 3H). ^{13}C-NMR (400 MHz, $CDCl_3$) δ166.7, 138.4, 136.5, 134.3, 115.0, 80.1, 61.4, 49.7, 32.0, 28.1, 21.0, 20.1, 13.9. LC-ESI-MS: 15.0 min, $[M+H]^+$=254. *S*-enantiomer $[\alpha]_D$= +19.5, *R*-enantiomer $[\alpha]_D$= -20.6 (*c* 1 in $CHCl_3$).

*(**8**)*

A $NaHCO_3$ (4 eq, 5.60 mmol) solution in water (2.5 ml), compound **7** (1 eq, 1.40 mmol) and Fmoc-Cl (1 eq, 1,4 mmol) were added to dioxane (1,4 ml) and the mixture was stirred at room temperature overnight. The reaction was quenched with water and the crude extracted with EtOAc and purified by flash chromatography (silica gel, 95:5=Cy:EtOAc), to isolate the products are yellow oils.

Yield of **(*S*)-8:** 90%. Yield of **(*R*)-8**: 89%.

Isomer a ^{1}H-NMR (400 MHz, $CDCl_3$) δ 7.73 (d, ^{3}J=7.2 Hz, 2H), 7.57 (dd, ^{3}J=7.6 Hz, ^{3}J=7.6 Hz, 2H), 7.36 (dd, ^{3}J=8.4 Hz, ^{3}J=8.4 Hz, 2H), 7.a30-7.24 (m, 2H), 6.83 (q, ^{3}J=7.2 Hz, 1H), 5.57 (m, 1H), 4.82 (m, 2H), 4.52 (m, 3H), 4.20 (m, 1H), 3.90 (m, 2H), 2.62 (m, 1H), 1.87 (d, ^{3}J=7.2 Hz, 3H), 1.45 (s, 9H), 0.82 (d, ^{3}J=6.4 Hz, 3H), 0.76 (d, ^{3}J=6.4 Hz, 3H). ^{13}C-NMR (400 MHz, $CDCl_3$, δ166.7, 156.8, 143.3, 142.9, 135.1, 134.6, 129.0, 127.5, 126.9, 124.9, 124.4, 118.8, 80.4, 66.8, 59.5, 47.5, 45.5, 28.0, 26.8, 20.0, 19.7, 14.5. **Isomer b** ^{1}H-NMR (400 MHz, $CDCl_3$) δ 7.73 (d, ^{3}J=7.2 Hz, 2H), 7.57 (dd, ^{3}J=7.6 Hz, ^{3}J=7.6 Hz, 2H), 7.36 (dd, ^{3}J=8.4 Hz, ^{3}J=8.4 Hz, 2H), 7.a30-7.24 (m, 2H), 6.62 (q, ^{3}J=7.2 Hz, 1H), 5.57 (m, 1H), 4.82 (m, 2H), 4.52 (m, 3H), 4.20 (m, 1H), 3.90 (m, 2H), 2.45 (m, 1H), 1.87 (d, ^{3}J=7.2 Hz, 3H), 1.45 (s, 9H), 0.82 (d, ^{3}J=6.4 Hz, 3H), 0.76 (d, ^{3}J=6.4 Hz, 3H). ^{13}C-NMR (400 MHz, $CDCl_3$,δ166.7, 156.8, 144.2, 142.7, 135.3, 133.5, 127.3, 126.9, 124.9, 124.4, 119.8, 80.3, 66.8, 66.1, 47.4, 45.8, 28.0, 27.3, 19.8, 19.2, 14.5. LC-ESI-MS: 19.0 min, 21.5 min, $[M+H]^+$=476, $[M+H]^+$=498. *S*-enantiomer $[\alpha]_D$= +6.38, *R*-enantiomer $[\alpha]_D$= -2.71 (*c* 1 in $CHCl_3$).

*(**9**)*

In a 2-necked round bottom flask, equipped to perform reaction under N_2 flow, enantiopure **8** (1 eq, 1.25 mmol) was dissolved in MTBE (6.25 ml) and Grubbs-II generation catalyst (0.03 eq, 0.04 mmol) was added. The mixture was stirred at 50 °C for 20 h. The reaction was quenched with vinilacetate and diluited with EtOAc. The organic layer was washed with water and concentrated under vacuum. The crude was purified by flash chromatography (silica gel, 98:2=Cy:EtOAc) to isolate the product as a single enantiomer.

Yield of **(*S*)-9**: 81%. Yield of **(*R*)-9**: 79%.

Isomer a: Transparent oil; ^{1}H-NMR (400 MHz, $CDCl_3$) δ7.75 (d, ^{3}J=6.8 Hz, 2H), 7.62-7.53 (m, 2H), 7.38 (dd, ^{3}J=7.6 Hz, ^{3}J=6.8 Hz, 2H), 7.31 (dd, ^{3}J=7.6 Hz, ^{3}J=7.2 Hz, 2H), 6.64 (m, 1H), 4.87 (m, 1H), 4.56 (d, ^{3}J=5.6 Hz, 2H), 4.55-4.22 (m, 3H), 2.30 (m, 1H), 1.48 (s, 9H), 0.93 (d, ^{3}J=6.8 Hz, 3H), 0.86 (d, ^{3}J=6.8 Hz, 3H). ^{13}C-NMR (400 MHz, $CDCl_3$)δ162.5, 155.0, 144.0, 143.8, 136.8, 136.0, 127.6, 124.9, 124.7, 119.9, 81.3, 68.8, 67.0, 54.2, 47.3, 32.5, 28.0, 19.0, 18.2. **Isomer b:** Transparent oil; ^{1}H-NMR (400 MHz, $CDCl_3$) δ7.75 (d, ^{3}J=6.8 Hz, 2H), 7.62-7.53 (m, 2H), 7.38 (dd, ^{3}J=7.6 Hz, ^{3}J=6.8 Hz, 2H), 7.31 (dd, ^{3}J=7.6 Hz, ^{3}J=7.2 Hz, 2H), 6.64 (m, 1H), 4.87 (m, 1H), 4.56 (d, ^{3}J=5.6 Hz, 2H), 4.55-4.22 (m, 3H), 1.89 (m, 1H), 1.48 (s, 9H), 0.73 (d, ^{3}J=6.8 Hz, 3H), 0.65 (d, ^{3}J=6.8 Hz, 3H). ^{13}C-NMR (400 MHz, $CDCl_3$)δ162.5, 154.8, 144.0, 143,8, 136.2, 135.6, 127.0, 124.9, 124.6, 119.9, 81.1, 68.4, 66.7, 53.9, 47.3, 32.2, 28.0, 17.8, 17.6. LC-ESI-MS: 15.6 min, $[M+H]^+$=434. *S*-enantiomer $[\alpha]_D$= -17.7, *R*-enantiomer $[\alpha]_D$= +26.5 (*c* 1 in $CHCl_3$).

*(**10**), (**23a**), (**26**), (**28**)*

Ester **9** or carbamate **22a**-**25**-**27** (1 eq, 1.01 mmol) was dissolved in DCM (10.1 ml) and TFA (15 eq, 15.21 mmol) was added at 0 °C. The mixture was stirred at room temperature overnight and then evaporated under vacuum. The product was used without further purifications.

Yield of **(*S*)-10, (*R*)-10**, **23a**, **26**, **28**: 99%

(10) Isomer a: Yellow oil; ^{1}H-NMR (400 MHz, $CDCl_3$) δ 7.76 (d, ^{3}J=7.6 Hz, 2H), 7.76-7.56 (m, 2H), 7.39 (dd, ^{3}J=7.2 Hz, ^{3}J=7.2 Hz, 2H), 7.32 (dd, ^{3}J=6.8 Hz, ^{3}J=6.8 Hz, 2H), 6.92 (m, 1H), 4.66 (d, ^{3}J=5.2 Hz, 1H), 4.56 (m, 1H), 4.43 (m, 1H), 4.33-4.20 (m, 2H), 4.09 (dd, ^{2}J=18.8 Hz, ^{3}J= 4.8 Hz, 1H), 2.30 (m, 1H), 0.94 (d, ^{3}J= 6.8 Hz, 3H), 0.84 (d, ^{3}J= 6.8 Hz, 3H). ^{13}C-NMR (400 MHz, $CDCl_3$) δ168.7, 156.1, 143.3, 141.4, 140.8, 133.2, 127.8, 127.1, 124.7, 120.0, 68.2, 67.8, 54.5, 47.1, 32.1, 18.9, 17.7. **Isomer b**: Yellow oil; ^{1}H-NMR (400 MHz, $CDCl_3$) δ 7.76 (d, ^{3}J=7.6 Hz, 2H), 7.76-7.56 (m, 2H), 7.39 (dd, ^{3}J=7.2 Hz, ^{3}J=7.2 Hz, 2H), 7.32 (dd, ^{3}J=6.8 Hz, ^{3}J=6.8 Hz, 2H), 6.92 (m, 1H), 4.66 (d, ^{3}J=5.2 Hz, 1H), 4.56 (m, 1H), 4.43 (m, 1H), 4.33-4.20 (m, 2H), 4.09 (dd, ^{2}J=18.8 Hz, ^{3}J= 4.8 Hz, 1H), 1.87 (m, 1H), 0.70 (d, ^{3}J= 6.8 Hz, 3H), 0.62 (d, ^{3}J= 6.8 Hz, 3H). ^{13}C-NMR (400 MHz, $CDCl_3$) δ168.7, 156.1, 143.1, 141.3, 140.5, 133.2, 127.8, 127.1, 124.6, 120.0, 68.2, 67.7, 54.2, 47.1, 32.1, 18.9, 17.7. LC (acid)-ESI-MS: 10.0 min, $[M+H]^+$=378. *S*-enantiomer $[\alpha]_D$= -22.22, *R*-enantiomer $[\alpha]_D$= +22.46 (*c* 1 in $CHCl_3$).

(23a): Sticky solid; ^{1}H-NMR (400 MHz, *d*-Acetone) δ7.56 (dd, ^{3}J=8.4 Hz, ^{4}J=1.6 Hz, 1H), 7.48 (dd, ^{3}J=13.6 Hz, ^{4}J=2 Hz, 1H), 7.18 (dd, ^{3}J=8.8 Hz, ^{3}J=8.8 Hz, 1H), 5.10 (m, 1H), 3.77 (d, ^{3}J=2 Hz, 1H), 3.57 (m, 8H), 3.20 (q, ^{3}J=7.2 Hz, 2H), 2.04 (m, 1H), 1.10 (t, ^{3}J=7.2 Hz, 3H), 1.03 (d, ^{3}J=6.8 Hz, 3H), 1.01 (d, ^{3}J=6.8 Hz, 3H). ^{13}C-NMR (400 MHz, *d*-Acetone) δ171.1, 171.6, 165.9, 154.8 (d, J=233 Hz), 142.7, 128.0 (d, J=8 Hz), 127.0 (d, J=3 Hz), 119.3 (d, J=3 Hz), 117.9 (d, J=23 Hz), 68.5, 50.7, 47.7, 44.3, 35.2 (d, J=13 Hz), 32.5, 18.4, 18.0, 14.6. LC-ESI-MS: 1.5 min, $[M+H]^+$=407, $[2M+H]^+$=813.

(26): Sticky solid;^{1}H-NMR (400 MHz, *d*-Acetone) δ 7.44 (d, ^{3}J=14.4 Hz, 1H), 7.36 (d, ^{3}J=13.2 Hz, 1H), 7.16 (dd, ^{3}J=8.8 Hz, ^{3}J=8.8 Hz, 1H), 6.37 (m, 1H), 5.43 (m, 1H), 4.52-4.47 (m, 2H), 4.03 (q, ^{3}J=7.2 Hz, 2H), 3.67-3.53 (m, 6H), 3.30-3.24 (m, 2H), 2.29 (m, 1H), 1.10 (t, ^{3}J=7.2 Hz, 3H), 0.98 (d, ^{3}J=6.8 Hz, 3H), 0.91 (d, ^{3}J=6.8 Hz, 3H). ^{13}C-NMR (400 MHz, *d*-Acetone) δ169.0, 163.4, 159.2, 140.5, 138.6, 131.2, 128.7, 124.6, 117.3, 114.4, 67.8, 57.4, 47.0, 43.8, 38.8, 33.73, 18.8, 17.0, 14.0. LC-ESI-MS: 1.5 min, $[M+H]^+$=390, $[2M+H]^+$=777. *S*-enantiomer $[\alpha]_D$= -38, *R*-enantiomer $[\alpha]_D$= +14 (*c* 1 in $CHCl_3$).

(28): Waxy solid; ^{1}H-NMR (400 MHz, CD_3OD) δ7.34 (d, ^{3}J=14 Hz, 1H), 7.31 (d, ^{3}J=18.4 Hz, 1H), 7.10 (dd, ^{3}J=8.4 Hz, ^{3}J=8.4 Hz, 1H), 6.34 (m, 1H), 5.43 (m, 1H), 5.48 (d, ^{3}J=16.4 Hz, 1H), 4.16 (d, ^{3}J=16.4 Hz, 2H), 3.98 (s, 2H), 3.78 (q, ^{3}J=7.2 Hz, 2H), 3.65-3.58 (m, 2H), 3.27- 3.16 (m, 6H), 2.29 (m, 1H), 1.13 (t, ^{3}J=7.2 Hz, 3H), 1.01 (d, ^{3}J=6.8 Hz, 3H), 0.94 (d, ^{3}J=6.8 Hz, 3H). ^{13}C-NMR (400 MHz, CD_3OD) δ169.7, 166.8, 163.1, 153.4, 141.1, 139.2, 130.5, 129.4, 124.2, 118.3, 117.0 (d, ^{3}J=22 Hz), 67.5, 57.7, 49.3, 38.5, 34.1, 29.2, 19.1, 17.5, 14.3. LC-ESI-MS: 1.6 min, $[M+H]^+$=446, $[M+Na]^+$=478. *S*-enantiomer $[\alpha]_D$= -17, *R*-enantiomer $[\alpha]_D$= +32 (*c* 1 in $CHCl_3$).

*(**11**)*

In a 2-necked round bottom flask, equipped to perform reaction under N_2 flow, **10** (1 eq, 1.01 mmol), TEA (1.5 eq, 1.52 mmol) and HBTU (1.5 eq, 1.52 mmol) were dissolved in dry DCM (13.5 ml). Ethylamine (2 eq, 2.02 mmol) was added and the mixture stirred overnight at room temperature. The reaction was quenched with water and the crude extracted with DCM. Purification by flash chromatography (silica gel, 6:4=Cy:EtOAc) allowed to isolate the product.

Yield of **(*S*)-11**: 98%. Yield of **(*R*)-11**: 96%.

Isomer a: Pale yellow oil; ^{1}H-NMR (400 MHz, $CDCl_3$) δ 7.75 (d, ^{3}J=7.2 Hz, 2H), 7.58 (d, ^{3}J=7.2 Hz, 2H), 7.47 (bs, 1H), 7.38 (dd, ^{3}J=7.2 Hz, ^{3}J=7.2 Hz, 2H), 7.30 (dd, ^{3}J=7.2 Hz, ^{3}J=7.2 Hz, 2H), 6.24 (m, 1H), 5.67 (m, 1H), 4.59 (d, ^{3}J=5.2 Hz, 1H), 4.48-4.21 (m, 3H), 4.05 (m, 1H), 3.34 (q, ^{3}J=7.2 Hz, 2H), 2.31 (m, 1H), 1.16 (t, ^{3}J=7.2 Hz, 3H), 0.70 (d, ^{3}J=6.8 Hz, 3H), 0.60 (d, ^{3}J=6.8 Hz, 3H). ^{13}C-NMR (400 MHz, $CDCl_3$) δ171.0, 154.8, 143.8, 141.3, 138.7, 138.5, 128.8, 127.6, 124.8, 124.5, 68.8, 66.9, 54.2, 47.3, 34.3, 31.8, 20.9, 14.5. LC-ESI-MS: 11.4 min $[M+H]^+$=405. **Isomer b:** Transparent oil; ^{1}H-NMR (400 MHz, $CDCl_3$) δ 7.75 (d, ^{3}J=7.2 Hz, 2H), 7.58 (d, ^{3}J=7.2 Hz, 2H), 7.47 (bs, 1H), 7.38 (dd, ^{3}J=7.2 Hz, ^{3}J=7.2 Hz, 2H), 7.30 (dd, ^{3}J=7.2 Hz, ^{3}J=7.2 Hz, 2H), 6.24 (m, 1H), 5.67 (m, 1H), 4.59 (d, ^{3}J=5.2 Hz, 1H), 4.48-4.21 (m, 3H), 4.05 (m, 1H), 3.34 (q, ^{3}J=7.2 Hz, 2H), 1.85 (m, 1H), 1.16 (t, ^{3}J=7.2 Hz, 3H), 0.70 (d, ^{3}J=6.8 Hz, 3H), 0.60 (d, ^{3}J=6.8 Hz, 3H). ^{13}C-NMR (400 MHz, $CDCl_3$) δ171.0, 154.5, 143.8, 141.2, 138.7, 138.5, 128.3, 126.9, 124.6, 119.8, 68.3, 66.5, 53.9, 47.2, 34.3, 32.1, 20.9, 14.0. LC-ESI-MS: 10.1 min $[M+H]^+$=405. *S*-enantiomer $[\alpha]_D$= -22.37, *R*-enantiomer $[\alpha]_D$= +25.81 (*c* 1 in $CHCl_3$).

*(**12**)*

Compound **11** (1 eq, 1.01 mmol) was dissolved in a 30% solution of piperidine in DMF (1.23 ml) and stirred at room temperature for 10 min. The reaction was quenched with water and the crude extracted with EtOAc. The crude was purified by flash chromatography (silica gel, 7:3=Cy:EtOAc) to isolate the product as pale yellow oil

Yield of **(*S*)-12**: 52%. Yield of **(*R*)-12**: 55%.

^{1}H-NMR (400 MHz, $CDCl_3$) δ 6.30 (m, 1H), 4.57 (bs, 1H), 4.14-4.03 (m, 2H), 3.34 (q, ^{3}J=7.2 Hz, 2H), 2.36 (m, 1H), 1.17 (t, ^{3}J=7.2 Hz, 3H), 1.06 (d, ^{3}J=7.2 Hz, 3H), 0.90 (d, ^{3}J=7.2 Hz, 3H). ^{13}C-NMR (400 MHz, $CDCl_3$) δ163.3, 143.1, 138.9, 70.3, 52.6, 34.3, 30.1, 19.4, 15.8. LC-ESI-MS: 1.7 min $[M+H]^+$=183. *S*-enantiomer $[\alpha]_D$= -23.3, *R*-enantiomer $[\alpha]_D$= +15.8 (*c* 1 in $CHCl_3$).

*(**13**)*

$SOCl_2$ (5 eq, 47.44 mmol) was added dropwise in MeOH (76 ml) at 0°C. After stirring for 15 min, 3,4-difluorobenzoic acid (1,5 g, 9.49 mmol) was added and the mixture was stirred at room temperature overnight. The solvent was removed under

vacuum e the product was used without further purifications (Y%=63%) as a waxy solid.

^{1}H-NMR (400 MHz, $CDCl_3$) δ 7.80 (m, 2H), 7.21 (dd, ^{3}J=8.4 Hz, ^{3}J=18 Hz, 1H), 3.91 (s, 3H). ^{13}C-NMR (400 MHz, $CDCl_3$) δ 164.5, 153.1 (dd, $^{2}J_{CF}$=13 Hz, $^{1}J_{CF}$=266 Hz), 149.6 (dd, $^{2}J_{CF}$=13 Hz, $^{1}J_{CF}$=247 Hz), 126.9 (dd, $^{4}J_{CF}$=13 Hz, $^{3}J_{CF}$=5 Hz), 126.1 (dd, $^{4}J_{CF}$=3 Hz, $^{3}J_{CF}$=7 Hz), 118.3 (d, $^{2}J_{CF}$=18 Hz), 116.8 (d, $^{2}J_{CF}$=18 Hz), 51.7. LC-ESI-MS: 8.3 min, $[M+H]^+$=173.

*(**14**), (**16**)*

13 (1,45 mmol), morpholine or piperazine (2 eq, 2.90 mmol) and K_2HPO_4 (4 eq, 5.80 mmol) were dissolvend in DMSO (4.4 ml) and the mixture was refluxed for 8 h. The solution was then poured into water and washed with EtOAc. The crude was purified by flash chromatography (silica gel, 8:2=Cy:EtOAc) to isolate the product.

Yield of **14**: 89%. Yield of **16**: 99%.

(14): Yellow oil; ^{1}H-NMR (400 MHz, $CDCl_3$) δ 7.74 (dd, ^{3}J= 31.6 Hz, ^{4}J=1.6 Hz, 1H), 7.72 (dd, ^{3}J= 36.8 Hz, ^{4}J=1.6 Hz, 1H), 6.94 (dd, ^{3}J=8.3 Hz, ^{3}J=8.3 Hz, 1H), 3.90 (s, 3H), 3.88 (t, ^{3}J= 4.8 Hz, 4H), 3.21 (t, ^{3}J=4.8 Hz, 4H). ^{13}C-NMR (400 MHz, $CDCl_3$) δ 165.7, 154.0 (d, $^{1}J_{CF}$=244 Hz), 143.0 (d, $^{2}J_{CF}$=8 Hz), 126.2 (d, $^{4}J_{CF}$=3 Hz), 123.2 (d, $^{3}J_{CF}$=8 Hz), 117.1 (d, $^{3}J_{CF}$=3 Hz), 117.1 (d, $^{2}J_{CF}$=22 Hz), 66.4, 51.7, 49.9. LC-ESI-MS: 7.7 min $[M+H]^+$=240.

(16): Yellow oil; ^{1}H-NMR (400 MHz, *d*-DMSO) δ 7.69 (dd, ^{3}J=31.6 Hz, ^{4}J=1.2 Hz, 1H), 7.66 (dd, ^{3}J=37.2 Hz, ^{4}J=1.2 Hz, 1H), 6.88 (dd, ^{3}J=8.4 Hz, 1H), 3.86 (s, 3H), 3.15 (t, ^{3}J=4.4 Hz, 2H), 3.02 (t, J=4.4 Hz, 2H), 2.58 (m, 4H). ^{13}C-NMR (400 MHz, *d*-DMSO) δ 163.6, 152.2 (d, $^{1}J_{CF}$=241 Hz), 142.8 (d, $^{2}J_{CF}$=7 Hz), 124.7 (d, $^{4}J_{CF}$=2 Hz), 120.8 (d, $^{3}J_{CF}$=8 Hz), 116.0 (d, $^{3}J_{CF}$=4 Hz), 115.2 (d, $^{2}J_{CF}$=4 Hz), 50.0, 44.2, 39.1. LC (acid)-ESI-MS: 1.3 min, $[M+H]^+$=239.

*(**15**), (**18**), (**20**)*

Esters **14** or **17** or **19** (1.29 mmol) was dissolved in a mixture 1:2=H_2O:THF (64.5 ml), then LiOH.H_2O (2 eq, 2.58 mmol) was added. The mixture was stirred overnight, acidified and the product extracted with EtOAc .

Yield of **15**: 99%. Yield of **18**, **20**: 99%.

(15): White solid, m.p. 199-201 °C; ^{1}H-NMR (400 MHz, *d*-DMSO) δ 7.62 (dd, ^{3}J=46 Hz, ^{4}J=1.6 Hz, 1H), 7.60 (dd, ^{3}J=51.6 Hz, ^{4}J=1.6 Hz, 1H), 7.06 (dd, ^{3}J=8.4 Hz, ^{3}J=8.4 Hz, 1H), 3.72 (t, ^{3}J=4.4 Hz, 2H), 3.11 (t, ^{3}J=4.4 Hz, 2H), 2.47 (m, 4H). ^{13}C-NMR (400 MHz, *d*-DMSO) δ 166.2, 153.5 (d, $^{1}J_{CF}$=243 Hz), 143.3 (d, $^{2}J_{CF}$=8 Hz), 126.4 (d, $^{4}J_{CF}$=3 Hz), 123.7 (d, $^{3}J_{CF}$=7 Hz), 118.1 (d, $^{3}J_{CF}$=3 Hz), 116.6 (d, $^{2}J_{CF}$=22 Hz), 66.9, 49.7. LC (acid)-ESI-MS: 3.0 min,$[M+H]^+$=226.

(18): White solid, m.p. 218-220 °C; ^{1}H-NMR (400 MHz, CDCl3) δ 7.69 (dd, ^{3}J=29 Hz, ^{4}J=1.6 Hz, 1H), 7.66 (dd, J=34.2 Hz, ^{4}J=1.6 Hz, 1H), 6.88 (dd, ^{3}J=6.8 Hz, ^{3}J=6.8 Hz, 1H), 3.15 (t, J=4.4 Hz, 4H), 3.02 (t, J=4.4 Hz, 4H), 1.45 (s, 9H). ^{13}C-NMR (400 MHz, $CDCl_3$) δ 170.4, 155.3, 152.9, 144.4, 127.8, 122.8, 117.9, 117.7, 80.2, 49.7, 49.6, 24,4. LC (acid)-ESI-MS: 6.3 min $[M+H]^+$=325.

(20): Pale yellow solid, m.p. 223-225 °C; ^{1}H-NMR (400 MHz, $CDCl_3$) δ 7.78 (d, ^{3}J=29.6 Hz, 2H), 7.76 (d, ^{3}J=34.4 Hz, 1H), 6.91 (dd, ^{3}J=8.4 Hz, ^{3}J=8.4 Hz, 1H), 5.56 (bs, 1H), 4.02 (s, 2H), 3.82-3.80 (m, 2H), 3.68 (t, ^{3}J= 4.8 Hz, 2H), 3.24 (t, ^{3}J=4.8 Hz, 2H), 3.21-3.19 (m, 2H), 1.45 (s, 9H). ^{13}C-NMR (400 MHz, $CDCl_3$) δ 169.5, 167.5, 155.6, 153.0, 144.1, 126.9, 123.6, 117.9, 117.8, 79.8, 66.6, 47.2, 38.4, 28.3. LC (acid)-ESI-MS: 7.9 min $[M+H]^+$=382.

*(**17**)*

In a 2-necked round-bottom flask, equipped to perform reaction under N_2 flow, Boc_2O (1 eq, 1.53 mmol) was dissolved in dry DCM (8.4 ml) and **16** (1.1 eq, 1.68 mmol) was added. TEA (1.5 eq, 2.30 mmol) was added dropwise at 0°C. The mixture was stirred at room temperature overnight, then poured into HCl 1M and extracted with DCM. The organic layer was washed with $NaHCO_3$ sat. sol. and brine. The yellow oil (Y%>99%) was used without further purifications.

^{1}H-NMR (400 MHz, $CDCl_3$) δ 7.70 (dd, ^{3}J= 29.6 Hz, ^{3}J=1.6 Hz, 1H), 7.68 (dd, ^{3}J= 34.8 Hz, ^{3}J=1.6 Hz, 1H), 6.88 (dd, ^{3}J=8.4 Hz, ^{3}J=6.8 Hz, 1H), 3.86 (s, 3H), 3.57 (t, ^{3}J= 4.8 Hz, 4H), 3.12 (t, ^{3}J= 4.8 Hz, 4H), 1.50 (s, 9H). ^{13}C-NMR (400 MHz, $CDCl_3$) δ165.3, 154.0, 153.8 (d, $^{1}J_{CF}$=246 Hz), 143.4 (d, $^{2}J_{CF}$=8 Hz), 126.0 (d, $^{4}J_{CF}$=3 Hz), 123.0 (d, $^{3}J_{CF}$=8 Hz), 117.5 (d, $^{3}J_{CF}$=3 Hz), 116.8 (d, $^{2}J_{CF}$=22 Hz), 79.3, 51.4, 49.3, 27.0. LC-ESI-MS: 11.1 min, $[M+H]^+$=339.

*(**19**)*

In a 2-necked round-bottom flask, equipped to perform reaction under N_2 flow, *N*-(Boc)-Gly-COOH (1 eq, 1,26 mmol) was dissolved in DMF (10.5 ml), COMU (1 eq, 1.26 mmol) and DIPEA (3 eq, 3.78 mmol) were added at 0°C. After stirring for 10 min, **18** (1 eq, 1.26 mmol) was added and mixture stirred at room temperature overnight. The reaction was quenched with HCl 1M and extracted with EtOAc. The organic layer was washed with $NaHCO_3$ saturated solution and with brine. The product (Y%>99%) was used without further purifications as a waxy solid.

^{1}H-NMR (400 MHz, $CDCl_3$) δ 7.72 (dd, ^{3}J= 27.2 Hz, ^{3}J=1.6 Hz, 1H), 7.70 (dd, ^{3}J= 32 Hz, ^{3}J=1.6 Hz, 1H), 6.88 (dd, ^{3}J=8.4 Hz, ^{3}J=8.4 Hz, 1H), 3.99 (s, 2H), 3.87 (s, 3H), 3.79 (t, ^{3}J= 5.2 Hz, 2H), 3.55 (t, ^{3}J= 5.2 Hz, 2H), 3.23-3.12 (m, 4H), 1.44 (s, 9H). ^{13}C-NMR (400 MHz, $CDCl_3$) δ166.7, 165.3, 162.1, 153.7 (d, $^{1}J_{CF}$=244 Hz), 142.8 (d, $^{2}J_{CF}$=9 Hz), 125.9 (d, $^{4}J_{CF}$=3 Hz), 123.4 (d, $^{3}J_{CF}$=7 Hz), 117.5 (d, $^{3}J_{CF}$=3 Hz), 116.8 (d, $^{2}J_{CF}$=22 Hz), 78.9, 66.0, 51.5, 46.7, 43.8, 27.7 . LC (acid)-ESI-MS: 8.2 min, $[M+H]^+$=396.

*(**21-a,b**), (**22a**), (**24**), (**25**), (**27**)*

In a 2-necked round bottom flask, equipped to perform reaction under N_2 flow, acid **15** or **18** or **20** (1.5 eq, 0.22 mmol) was dissolved in dry DCM (35 ml) and thionyl chloride (1.5 eq, 0.22 mmol) was added dropwise at 0 °C. The mixture was stirred at room temperature for 1 h and pyridine (5 eq, 0.75 mmol) was added. The mixture was stirred for 30 min and cyclic amine **3a** or **3b** or **(S)-12** or **(R)-12** (1 eq, 0.15 mmol) was added. The reaction was stirred for 3 h and then quenched with water and extracted with DCM. The crude was purified by flash chromatography (silica gel, 1:1=Cy:EtOAc) to isolate the product.

Yield of **21a**: 90%. Yield of **21b**: 90%. Yield of **22a**: 87%. Yield of **24**: 88%. Yield of **25**: 93%. Yield of **27**: 90%.

(21a): Yellow oil; ^{1}H-NMR (400 MHz, $CDCl_3$) δ 7.55 (dd, ^{3}J= 22.4, ^{4}J= 1.6 Hz, 1H), 7.52 (dd, ^{3}J= 27.6 Hz, ^{4}J= 1.6 Hz, 1H), 6.98 (dd, ^{3}J= 8.4 Hz, ^{3}J=8.4 Hz, 1H), 6.13 (bs, 1H), 5.27 (dd, ^{3}J=28 Hz, ^{3}J=6 Hz, 1H), 3.88 (t, ^{3}J= 4.4 Hz, 4H), 3.40 (d, ^{3}J= 28 Hz, 1H), 3.33-3.16 (m, 6H), 2.14 (m, 1H), 1.13 (t, ^{3}J=7.2 Hz, 3H), 1.03 (d, ^{3}J=6.8 Hz, 6H). ^{13}C-NMR (400 MHz, $CDCl_3$) δ171.4, 171.1, 162.4, 153.9 (d, ^{1}J=245 Hz), 143.3 (d, ^{3}J=8 Hz), 126.4 (d, ^{3}J=4 Hz), 124.7 (d, ^{2}J=13 Hz), 117.5 (d, ^{2}J=24 Hz), 117.3 (d, ^{3}J=4 Hz), 66.6, 66.0, 50.1, 50.0, 49.6, 35.2, 31.5, 17.9, 17.8, 14.3. LC-ESI-MS: 8.5 min, $[M+H]^+$=408, $[M+Na]^+$=430.

(21b): Yellow oil; ^{1}H-NMR (400 MHz, $CDCl_3$) δ7.54 (dd, ^{3}J=23.6 Hz, ^{4}J=2 Hz, 1H), 7.51 (dd, ^{3}J=28.8 Hz, ^{4}J=2 Hz, 1H), 6.90 (dd, ^{3}J=8.4 Hz, ^{3}J=8.4 Hz, 1H), 6.12 (bs, 1H), 5.25 (dd, ^{3}J=6 Hz, ^{3}J=28 Hz, 1H), 3.86 (t, ^{3}J=4.8 Hz, 4H), 3.44 (d, ^{3}J=28 Hz, 1H), 3.36-3.13 (m, 6H), 1.80 (m, 1H), 1.32-1.05 (m, 5H), 1.12 (t, ^{3}J=7.2 Hz, 3H), 0.89-0.82 (m, 5H). ^{13}C-NMR (400 MHz, $CDCl_3$) δ171.6, 171.1, 162.8, 153,6 (d, ^{1}J=245 Hz), 143.2 (d, ^{2}J=8 Hz), 126.4 (d, ^{3}J=3 Hz), 124.9, 117.6 (d, ^{2}J=23 Hz), 117.3 (d, ^{3}J=4 Hz), 66.7, 65.7, 50.1, 49.9, 41.2, 35.2, 28.5, 28.3, 25.9, 25.6, 14.2. LC-ESI-MS: 10.3 min, $[M+H]^+$=448, $[M+K]^+$=486, $[2M+Na]^+$=917.

(22a): Dark yellow oil; ^{1}H-NMR (400 MHz, $CDCl_3$) δ7.54 (d, ^{3}J=20.4 Hz, 1H), 7.51 (d, ^{3}J=25.2 Hz, 1H), 6.90 (dd, ^{3}J=8.4 Hz, ^{3}J=8.4 Hz, 1H), 6.15 (bs, 1H), 5.26 (dd, ^{3}J=28 Hz, ^{3}J=6 Hz, 1H), 3.58 (m, 4H), 3.34-3.25 (m, 2H), 3.16-3.09 (m, 4H), 2.12 (m, 1H), 1.46 (s, 9H), 1.12 (t, ^{3}J=7.2 Hz, 3H), 1.02 (d, ^{3}J=6.8 Hz, 6H). ^{13}C-NMR (400 MHz, $CDCl_3$) δ171.6, 171.0, 162.1, 154.6, 154.0 (d, ^{1}J=144 Hz), 143.4 (d, ^{3}J=8 Hz), 126.4 (d, ^{3}J=3 Hz), 124.9 (d, ^{3}J=8 Hz), 117.8 (d, ^{3}J=3 Hz), 117.6 (d, ^{2}J=24 Hz), 80.0, 65.9, 49.7 (d, ^{3}J=4 Hz), 49.6, 35.3, 31.6, 28.3, 18.0, 17.8, 14.4. LC-ESI-MS: 11.0 min, $[M+H]^+$=507, $[M+Na]^+$=529, $[M+K]^+$=545.

(24): Yellow oil; ^{1}H-NMR (400 MHz, $CDCl_3$) δ7.46 (bs, 1H), 7.36 (d, ^{3}J=24.8 Hz, 1H), 7.34 (d, ^{3}J=30 Hz, 1H), 7.05 (dd, ^{3}J=8.4 Hz, ^{3}J=8.4 Hz, 1H), 6.37 (m, 1H), 5.44 (m, 1H), 4.49 (d, ^{3}J=15.6 Hz, 1H), 4.17 (d, ^{3}J=16.4 Hz, 1H), 3.78 (t, ^{3}J=4.4 Hz, 4H), 3.26 (m, 2H), 3.16-3.07 (m, 4H), 2.28 (m, 1H), 1.10 (t, ^{3}J=7.2 Hz, 3H), 0.97 (d, ^{3}J=6.8 Hz, 3H), 0.90 (d, ^{3}J=6.8 Hz, 3H). ^{13}C-NMR (400 MHz, $CDCl_3$) δ169.8, 163.3, 154.5 (d, ^{1}J=247 Hz), 141.9 (d, ^{3}J=8 Hz), 139.1, 135.1, 129.4, 124.6 (d, ^{2}J=60 Hz), 117.8, 116.0 (d, ^{2}J=24 Hz), 67.6, 66.7, 57.4, 50.3, 34.3, 32.7, 19.3, 17.6, 14.6. LC-ESI-MS: 11.5 min, $[M+H]^+$=390, $[2M+Na]^+$=412. *S*-enantiomer $[\alpha]_D$= -58, *R*-enantiomer $[\alpha]_D$= +41 (*c* 1 in $CHCl_3$).

(25): Transparent oil; ^{1}H-NMR (400 MHz, $CDCl_3$) δ7.28 (dd, ^{3}J=13.6 Hz, ^{4}J=1.6 Hz, 1H), 7.25 (dd, ^{3}J=18 Hz, ^{3}J=1.6 Hz, 1H), 6.90 (dd, ^{3}J=8.4 Hz, ^{3}J=8.4 Hz, 1H), 6.33 (m, 1H), 5.78 (bs, 1H), 5.47 (m, 1H), 4.36 (d, J=14.4 Hz, 1H), 4.16 (d, ^{3}J=14.8 Hz, 1H), 3.58 (t, ^{3}J=5.2 Hz, 4H), 3.38-3-31 (m, 2H), 3.13-3.05 (m, 4H), 2.31 (m, 1H), 1.49 (s, 9H), 1.16 (t. ^{3}J=7.2 Hz, 3H), 1.02 (d, ^{3}J=7.2 Hz, 3H), 0.94 (d, J=7.2 Hz, 3H). ^{13}C-NMR (400 MHz, $CDCl_3$) δ169.7, 163.3, 155.8, 154.6, 142.0, 139.1, 129.7, 129.4, 124.3, 118.3, 116.0, 79.9, 67.6, 57.4, 50.0, 34.3, 29.2, 28.4, 17.6, 14.6. LC-ESI-MS: 9.3 min, $[M+H]^+$=489, $[M+Na]^+$=511, $[M+K]^+$=527, $[2M+H]^+$=976, $[2M+Na]^+$=999. *S*-enantiomer $[\alpha]_D$= -47, *R*-enantiomer $[\alpha]_D$= +40 (*c* 1 in $CHCl_3$).

(27): Transparent oil; ^{1}H-NMR (400 MHz, $CDCl_3$) δ7.30-7.27 (m, 2H), 6.89 (dd, ^{3}J=8.4 Hz, ^{3}J=8.4 Hz, 1H), 6.33 (m, 1H), 5.73 (bs, 1H), 5.47 (m, 1H), 4.36 (dd, ^{3}J=16.4 Hz, ^{3}J=3.6 Hz, 1H), 4.15 (d, ^{3}J=15.6 Hz, 1H), 3.99 (d, ^{3}J=4.4 Hz, 2H), 3.80-3.78 (m, 2H), 3.57-3.54 (m, 2H), 3.39-3-32 (m, 2H), 3.14-3.07 (m, 4H), 2.33 (m, 1H), 1.44 (s, 9H), 1.16 (t, ^{3}J=7.2 Hz, 3H), 1.02 (d, ^{3}J=7.2 Hz, 3H), 0.94 (d, ^{3}J=7.2 Hz, 3H).^{13}C-NMR (400 MHz, $CDCl_3$) δ169.6, 166.9, 163.3, 155.7, 153.4, 141.3, 139.1 130.3, 129.3, 124.3, 118.4, 116.0 (d, ^{3}J=22 Hz), 79.7, 67.6, 66.6, 57.4, 49.7, 44.3, 34.3, 29.6, 28.3, 19.3, 17.8, 14.6. LC-ESI-MS: 7.27 min, $[M+H]^+$=546, $[2M+Na]^+$=569. *S*-enantiomer $[\alpha]_D$= -30, *R*-enantiomer $[\alpha]_D$= +31 (*c* 1 in $CHCl_3$).

4.3 Antibacterial activity assay

4.3.1 Bacterial strains

A total of 12 well-characterized for their antibiotic-susceptibility phenotype *S. aureus* recently isolated strains, both MRSA and MSSA, were used for the determination of the *in vitro* antibacterial activity of the studied compounds. *Staphylococcus aureus* ATCC 29213 and *E. faecalis* ATCC 29212 reference standard strains were used as control.

4.3.2 Determination of MICs

The *in vitro* antibacterial activity of the new synthetized compounds (**21a**, **21b**, (***S***)-**24**, (***R***)-**24**) was studied by determining their minimum inhibitory concentrations (MICs) by means of the broth microdilution method according to the Clinical and Laboratory Standards Institute (CLSI) guidelines.[37] Linezolid (Sigma Aldrich, Italy) was used as reference antibiotic compound for MIC determinations.

Briefly, serial 2-fold dilutions of each compound were made using the Mueller-Hinton broth in microtitre plates with 96 wells. Dimethyl sulfoxide (DMSO) was used as solvent for all the synthetized compounds. An equal volume of the bacterial inoculum

(1x10^6 CFU/mL) was added to each well on the microtitre plate containing 0.05 mL of the serial antibiotic dilutions. The microtitre

plate was then incubated at 37 C for 18-24 h after which each well

was analyzed for the presence of bacterial growth. The MIC was

defined as the lowest concentration of antimicrobial agent able to

cause inhibition of bacterial growth as shown by the lack of visible turbidity of the culture medium.

4.4 Cell cultures conditions

The effects of synthetized compounds (**21a**, **21b**, **(*R*)-24** and **(*S*)-24**) and Linezolid on cells viability and MAO activity were studied in vitro on HepG2 cells, (human hepatocellular carcinoma). Cells were grown in Dulbecco's modified eagles medium (DMEM) supplemented with 10% heat inactivated foetal bovine serum (FBS), 2mM L-glutamine, 100 units/ml penicillin and 100µg/ml streptomycin and maintained on collagen coated 75-cm^2 flask at 37°C in a 5% CO_2 atmosphere. All reagents for cell culture were from Euroclone, Pero, Italy.

4.5 Cell viability assay

Cells were seeded at 45,000 cell/cm^2 onto collagen coated 24-well plates, and after two days treated with increasing concentrations (10-100µg/mL) of **21a**, **21b**, **(*R*)-24** and **(*S*)-24** compounds. After 24 h treatment, cell viability was evaluated by means of PrestoBlue® Cell Viability Reagent, a cell permeable resazurin-based solution that modified by the reducing power of living cells turns red in colour. Briefly, PrestoBlue® was administrated to cells according to the manufacturer's protocol and incubated for 1 h at 37°C. The absorbance was measured with FLUOstar Omega (BMG Labtech) multidetection microplate reader at wavelength of 570 nm and at reference wavelength of 600nm. The same assay was performed in cells treated with 100µg/mL of Linezolid. All data are expressed as mean ± SEM of three separate experiments performed in triplicate. The differences were calculated by means of Student's t test. A p value <0.05 was considered to be statistically significant.

4.6 MAO activity assay

Cells were seeded at 45,000 cell/cm^2 onto collagen coated 24-well plates, and after two days treated with **21a**, **21b**, **(*R*)-24** and **(*S*)-24** compounds with increasing concentrations (10-100µg/mL). After 24 h treatment cells were harvested and lysed with a non-denaturizing buffer (10mM Tris pH 7.5, 100mM NaCl, 1mM EDTA, 0.01% Triton X-100). Then cells were completely disrupted by sonication with an Ultrasonic Sonicator bath 2510 (Branson). MAO inhibition was evaluated by means of Amplex® Red Monoamine oxidase Assay kit, a one-step colorimetric method based on the detection of H_2O_2 in a horseradish peroxidase coupled reaction using 10-acetyl-3,7-dihydroxyphenoxazine (amplex red reagent) a highly sensitive stable probe for H_2O_2. Briefly, according to manufacturer's protocol, samples were incubated with Amplex Red working solutions for 30 minutes at room temperature. The absorbance was measured with a multilabel Victor3 spectrophotometer (Perkin Elmer) at wavelength of 570 nm. The same assay was performed in cells treated with 100µg/mL of Linezolid. All data are expressed as mean ± SEM of three separate experiments performed in triplicate. The differences were calculated by means of Student's t test. A p value <0.05 was considered to be statistically significant.

4.7 Docking studies

Docking studies on human MAO-A were done on the high resolution 2Z5X structure bound with the reversible inhibitor harmine,[33] while the high resolution 2V5Z structure bound with safinamide was used for human MAO-B studies.[34] In both cases, the pdb files were prepared for docking using the Schrödinger Protein Preparation Wizard.[35] Crystallization supplementary ligands and water molecules were removed from structure, hydrogens were added and missing side-chains and loops were filled in. In the case of 2V5Z heterodimer, only chain A was used. Finally, the protein was refined with an energy-restrained minimization, using OPLS-2005 force field. The optimized pdb files were subjected to docking with AutoDock Vina [36] and PyMOL,[38] using the PyMOL Autodock plugin.[39] The centroid of the co-crystallized ligands was used to set up the docking grid cube of size 22.5 Å. In all cases, the validity of the obtained receptor was tested re-docking the original co-crystallized ligand, obtaining an RMS of 0.313 for harmine and MAO-A and an RMS of 1.716 for safinamide and MAO-B. Figures were produced using PyMOL.

Acknowledgements

This study has been carried out with the fundamental contribution of "Fondazione del Monte di Bologna e Ravenna", MIUR and University of Bologna. Mr. Andrea Garelli is gratefully acknowledged for the LC-ESI-MS analysis.

References

[1] Food and Drugs Consumer Health Informations, November 2013.

[2] K.J. Shaw, M.R. Barbachyn, The oxazolidinones: past, present and future, Ann. N. Y. Acad. Sci., 2011, 1241, 48-70.

[3] P.W. Ament, N. Jamshed, J.P. Horne, Linezolid: Its Role in the Treatment of Gram-Positive, Drug-Resistant Bacterial InfectionsAm. Fam. Physician, 2002, 65, 663-670.

[4] D.N. Wilson, F. Schluenzen, J.M. Harms, A.L. Starosta, S.R. Connell, P. Fucini, The oxazolidinone antibiotics perturb the ribosomal peptidyl-transferase center and effect tRNA positioning, PNAS, 2008, 105 (36), 13339-13344

[5] S.J. Brickner, M.R. Barbachyn, D.K. Hutchinson, P.R. Manninen, Linezolid (ZYVOX), the First Member of a Completely New Class of Antibacterial Agents for Treatment of Serious Gram-Positive Infections, J. Med. Chem., 2008, 51 (12), 3353-3356

[6] A.C. Gales, H.S. Sader, S.S. Andrade, L.Lutz, A. Machadoc, A.L. Barth, Emergence of linezolid-resistant Staphylococcus aureus during treatment of pulmonary infection in a patient with cystic fibrosis, Int. J. Antimicrob. Agents, 2006, 27, 300-302

[7] M.R. Barbachyn, G.J. Cleek, L.A. Dolak, S.A. Garmon, J. Morris, E.P. Seest, R.C. Thomas, D.S. Toops, W.Watt, D.G. Wishka, C.W. Ford, G.E. Zurenko, J.C. Hamel, R.D. Schaadt, D. Stapert, B.H. Yagi, W.J. Adams, J.M. Friis, J.G. Slatter, J.P. Sams, N.L. Oien, M.J. Zaya, L.C. Wienkers, M.A. Wynalda, Identification of Phenylisoxazolines as Novel and Viable Antibacterial Agents Active against Gram-Positive Pathogens, J. Med. Chem, 2003, 46, 284-302.

[8] Denis, A.; Villette, T. 5-Aryl-â,ç Butenolide, a New Class of Antibacterial Derived from the N-Aryl Oxazolidinone DUP 721. Bioorg. Med. Chem. Lett. 1994, 4, 1925-1930.

[9] Borthwick, A. D.; Biggadike, K.; Rocherolle, V.; Cox, D. M.; Chung, G. A. C., 5-(Acetamidomethyl)-3-aryldihydrofuran-2-ones and 5-(Acetamidomethyl)-3-aryltetrahydrofuran-2-ones, Two New Classes of Antibacterial Agents. Med. Chem. Res. 1996, 6, 22-27.

[10] A.Renslo, G.W. Luehr, M.F. Gordeev, Recent developments in the identification of novel oxazolidinone antibacterial agents, Bioorg. Med. Chem., 2006, 14, 4227-4240.

[11] A. Palumbo Piccionello, R. Musumeci, C. Cocuzza, C.G. Fortuna, A. Guarcello, P. Pierro, A. Pace, Synthesis and preliminary antibacterial evaluation of Linezolid-like 1,2,4-oxadiazole derivatives, Eur. J. Med. Chem., 2012, 50, 441-448.

[12] O.A. Phillips, R. D'Silva, T.O. Bahta, L.H. Sharaf, E.E. Udo, L. Benov, D.E. Walters, Synthesis and biological evaluation of novel 5-(hydroxamic acid) methyl oxazolidinone derivatives, Eur. J. Med. Chem, 2015, 106, 120-131.

[13] J.G. Slatter, D.J. Stalker, K.L. Feenstra, I.R. Welshman, J.B. Bruss, J.P. Sams, M.G. Johnson, P.E. Sanders, M.J. Hauer, P.E. Fagemess, R.P. Styd, G.W. Peng, E.M. Shobe, Pharmacokinetics, methabolism and excretion of linezolid following an oral dose of [^{14}C] linezolid to healthy human subjects, Drug. Metab. Dispos., 2001, 29, 1136-1145.

[14] M.A. Wynalda, M.J. Hauer, L.C. Wienkers, Oxidation of novel oxazolidinone antibiotic linezolid in human liver microsomes, Drug. Metab. Dispos. 2000, 20, 1014-1017.

[15] M.E. Brier, D.J. Stalker, G.R. Aronoff, D.H. Batts, K.K. Ryan, M. O'Grady, N.K. Hopkins, G.L. Junglubuth, Pharmacokinetics of linezolid in subjects with renal dysfunctions, Antimicro. Agents Chemoth. 2003, 47, 2775-2780

[16] J. Wouters, F. Moureau, G. Evrard, J. Koenig, S. Jegham, P. George, F. Durant, A Reversible Monoamine Oxidase A Inhibitor, Be¯oxatone: Structural Approach of its Mechanism of Action, Bioorg. Med. Chem., 1999, 7, 1683-1693.

[17] P. Riederer, W. Danielczyk, E. Grunblatt Monoamino Oxidase-B Inhibition in Alzheimer's Disease, NeuroToxycology, 2004, 25, 271-277.

[18] T.Z.E. Jones, P. Fleming, C.J. Eyermann, M.B. Gravestock, R.R. Ramsay, Orientation of oxazolidinones in the active site of monoamine oxidase, Biochemical Pharmacology, 2005, 70, 407–416.

[19] K.R. Lawrence, M. Adra, P.K. Gillman, Serotonin Toxicity Associated with the Use of Linezolid: A Review of Postmarketing Data, Clin. Infect. Dis., 2006, 42, 1578-1583.

[20] C. Binda, M. Li, F. Huba´ lek, N. Restelli, D.E. Edmondson, A. Mattevi, Insights into the mode of inhibition of human mitochondrial monoamine oxidase B from high-resolution crystal structures, Proc. Natl. Acad. Sci. USA 2003, 100, 9750–9755.

[21] T. Poel, R.C. Thomas, W.J. Adams, P.A. Aristoff, M.R. Barbachyn, F.E. Boyer, J.Brieland, R. Brideau, J. Brodfuehrer, A.P. Brown, A.L. Choy, M.Dermyer, M.Dority, C.W. Ford, R.C. Gadwood, D. Hanna, C. Hongliang, M.D. Huband, C. Huber, R. Kelly, J. Kim, J.P. Martin, Jr., P.J. Pagano, D.Ross, L. Skerlos, M.C. Sulavik, T. Zhu, G.E. Zurenko, J. V. N. V. Prasad, Antibacterial Oxazolidinones Possessing a Novel C-5 Side Chain. (5R)-trans-3-[3-Fluoro-4-(1-oxotetrahydrothiopyran-4-yl)phenyl]-2-oxooxazolidine-5-carboxylic Acid Amide (PF-00422602), a New Lead Compound, J. Med. Chem., 2007, 50, 5886-5889.

[22] A. Tolomelli, M. Baiula, A. Viola, L. Ferrazzano, L. Gentilucci, S. D. Dattoli, S. Spampinato, E. Juaristi, M. Escudero, Dehydro-β-proline Containing α4β1 Integrin Antagonists: Stereochemical Recognition in Ligand−Receptor Interplay, ACS Med. Chem. Lett., 2015, 6, 701-706.

[23] G. Cardillo, L. Gentilucci, M. Gianotti, R. Perciaccante, A. Tolomelli, Synthesis of Aziridine-2,2-dicarboxylates via 1,4-Addition of N,O-(Bistrimethylsilyl)hydroxylamine to α,β-Unsaturated Malonates, JOC, 2001, 66, 8657-8660.

[24] A. Tolomelli, G. Cardillo, L. Gentilucci, R. Juris, A. Viola, E. Juaristi, Exploring the reactivity of alkylidene malonamides: synthesis of polyfunctionalized isoxazolidinones, aziridines and oxazoline, Arkivoc, 2012, v, 196-209.

[25] G. Cardillo, L. Gentilucci, M. Gianotti, H. Kim, R. Perciaccante, A. Tolomelli, Conjugate addition of hydroxylamino derivatives to alkylidene malonates in the presence of chiral Lewis acid, Tetrahedron Asymmetry.

[26] A. Tolomelli, L. Gentilucci, E. Mosconi, A. Viola, E. Paradisi, A straightforward route to enantiopure 2-substituted-3,4-dehydro-b-proline via ring closing metathesis, Amino Acids (2011), 41, 575–586.

[27] A. Tolomelli, M. Baiula, A. Viola, L. Ferrazzano, L. Gentilucci, S.D. Dattoli, S. Spampinato, E. Juaristi, M. Escudero, Dehydro-β-proline Containing α4β1 Integrin Antagonists: Stereochemical Recognition in Ligand−Receptor Interplay, ACS Med. Chem. Lett. 2015, 6, 701−706.

[28] J. Grimsby, N.C. Lan, R. Neve, K. Chen, J.C. Shih, Tissue distribution of human monoamine oxidase A and B Mrna, J. Neurochem. 1990, 55, 1166–1169.

[29] S.D. Sivasubramaniam, C.C. Finch, M.J. Rodriguez, N. Mahy, E.E. Billett, A comparative study of the expression of monoamine oxidase-A and -B mRNA and protein in non-CNS human tissues, Cell Tissue Res. 2003, 313 (3), 291-300.

[30] C.G. Fortuna, R. Berardozzi, C. Bonaccorso, G. Caltabiano, L. Di Bari, L. Goracci, A. Guarcello, A. Pace, A. Palumbo Piccionello, G. Pescitelli, P. Pierro, E. Lonati, A. Bulbarelli, C.E. Cocuzza, G. Musumarra, R. Musumeci, New potent antibacterials against Gram-positive multiresistant pathogens: effects of side chain modification and chirality in linezolid-like 1,2,4-oxadiazoles, Bioorg Med Chem. 2014, 22(24), 6814-6825.

[31] S.-Y. Son, J. Ma, Y. Kondou, M. Yoshimura, E. Yamashita, T. Tsukihara, Structure of human monoamine oxidase A at 2.2-Å resolution: The control of opening the entry for substrates/inhibitors, PNAS 2008, 105, 5739−5744.

[32] C. Binda, P. Newton-Vinson, F. Hubálek, D. E. Edmondson, A. Mattevi, Structure of human monoamine oxidase B, a drug target for the treatment of neurological disorders, Nat. Struct. Biol. 2002, 9, 22−26.

[33] 2Z5X: www.rcsb.org/pdb/explore.do?structureId=2z5x (2.2 Å resolution). Crystal Structure of Human Monoamine Oxidase A with Harmine.

[34] 2V5Z: www.rcsb.org/pdb/explore/explore.do?structureId=2v5z (1.6 Å resolution). Structure of Human Mao B in Complex with the Selective Inhibitor Safinamide.

[35] Protein Preparation Wizard 2015-2; Epik version 2.4, Schrödinger, LLC, New York, NY, 2015; Impact version 5.9, Schrödinger, LLC, New York, NY, 2015; Prime version 3.2, Schrödinger, LLC, New York, NY, 2015. G. M. Sastry, M. Adzhigirey, T. Day, R. Annabhimoju, W. Sherman, Protein and ligand preparation: parameters, protocols, and influence on virtual screening enrichment, J. Comput. Aided Mol. Des. 2013, 27, 221−234.

[36] O. Trott, A. J. Olson, AutoDock Vina: Improving the speed and accuracy of docking with a new scoring function, efficient optimization, and multithreading, J. Comput. Chem. 2010, 31, 455–461.

[37] Clinical and Laboratory Standards Institute. Approved Standard, Methods for Dilution Antimicrobial Susceptibility Tests for Bacteria That Grow Aerobically, ninth ed., vol. 32, M07eA9, Wayne, Pennsylvania, 2011.

[38] The PyMOL Molecular Graphics System, Version 1.8 Schrödinger, LLC.

[39] wwwuser.gwdg.de/~dseelig/adplugin.html.

Graphical Abstract

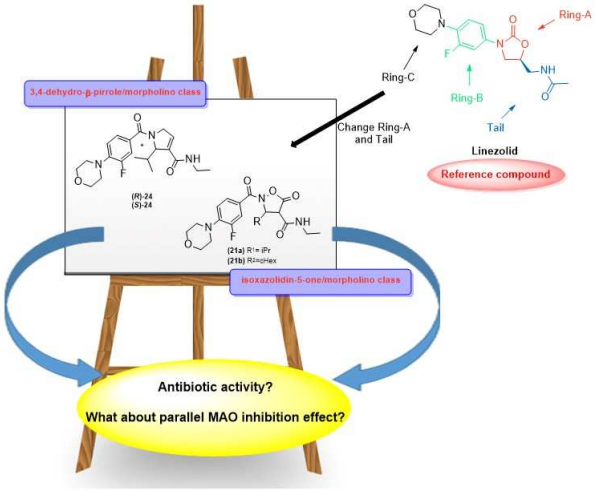

New isoxazolidinone and 3,4-dehydro-β-proline derivatives as antibacterial agents and MAO-inhibitors: a complex balance between two activities.

Lucia Ferrazzano[a], Angelo Viola[a], Elena Lonati[b], Alessandra Bulbarelli[b], Rosario Musumeci[b], Clementina Cocuzza[b], Marco Lombardo[a], Alessandra Tolomelli[a]*

Highlights

- The synthesis of novel Linezolid-like derivatives has been carried out
- Isoxazolidinone and 3,4-dehydro-β-proline rings were used as scaffolds
- Antibacterial activity was modest but a good affinity for MAO-A and B was observed
- Docking experiments suggest a particular affinity for MAO-B